hypothesized to result in protein truncation due to abnormal splicing. Further analysis of 19 unrelated probands unlinked to *FBN1* identified c.923T > C (p.L308P), c.1346C > T (p.S449F) and c.1609C > T (p.R537C; recurrent in two independent families) (Table 2 and Fig. 1). These missense mutations affect an evolutionarily conserved amino acid in the serine/threonine kinase domain of TGFβ receptor type II. This finding confirmed that the MFS phenotype can be caused not only by mutations in *FBN1* but also by mutations in *TGFBR2*.

Loeys–Dietz syndrome

Loeys et al. (2005) reported a new aortic aneurysm syndrome presenting with cardiovascular and skeletal manifestations consistent with those seen in MFS, along with other features not present in MFS. Loeys–Dietz syndrome (LDS, OMIM #609192) is characterized by hypertelorism, bifid uvula, cleft palate, generalized arterial tortuosity, and ascending aortic aneurysm and dissection. Hypothesizing that abnormal TGFβ signaling might cause vascular and craniofacial phenotypes, Loeys et al. (2005) investigated *TGFBR2* as a candidate gene for LDS. Heterozygous *TGFBR2* mutations were found in six of ten LDS patients: five missense mutations in the serine/threonine kinase domain [c.1006T > A (p.Y336N), c.1063G > C (p.A355P), c.1069G > T (p.G357W), c.1582C > T (p.R528C), c.1583G > A (p.R528H)], as seen in MFS2, and a single mutation in a splice-acceptor site (IVS1-2A > G) (Table 2, Fig. 1). The remaining four patients were shown to have *TGFBR1* mutations: three missense mutations in the serine/threonine kinase domain [c.953T > G (p.M318R), c.1199A > G (p.D400G) and c.1460G > C (p.R487P)] and a missense mutation in the glycine/serine-rich (GS) domain [c.599C > T (p.T200I)] (Table 2, Fig. 1). Owing to the clinical overlap of MFS and Shprintzen–Goldberg craniosynostosis syndrome (SGS) with LDS, Loeys et al. (2005) also screened seven MFS patients (unlinked to *FBN1*) and five SGS patients for mutations in *TGFBR1* and *TGFBR2*, but no abnormalities were seen at these loci.

Two other *TGFBR2* mutations [c.773T > G (p.V258G) and c.1067G > C (p.R356P)] and another *TGFBR1* mutation [c.722C > T (p.S241L)] have since been reported in other patients meeting the clinical description of LDS by other groups (Table 2, Fig. 1) (Ki et al. 2005; Matyas et al. 2006). Finally, Loeys et al. (2006) collected 30 more probands of LDS and found *TGFBR2* mutations in 21 and *TGFBR1* mutations in nine (Table 2, Fig. 1) (Loeys et al. 2006). Furthermore, LDS type II (LDS2) without craniofacial features was also proposed. Eight *TGFBR2* and four *TGFBR1* mutations were found in LDS2 patients (Tables 2 and 3, Fig. 1) (Loeys et al. 2006).

Familial thoracic aortic aneurysms and dissections

Non-syndromic thoracic aortic aneurysms and dissections (TAAD) have complex and heterogeneous etiology, with some families inheriting TAAD in an autosomal dominant fashion, with decreased penetrance and variable expression. To date, at least three TAAD loci have been mapped by linkage studies of large single families (Pannu et al. 2005b): *TAAD1* at 5q13–q14 (Guo et al. 2001), the familial aortic aneurysm 1 locus (*FAA1*) at 11q23–q24 (Vaughan et al. 2001), and *TAAD2* at 3p24–p25 (Hasham et al. 2003).

The realization that TAAD2 (OMIM, #608987) and MFS2 are clinically overlapping diseases that both map to 3p24–p25 led Pannu et al. (2005a) to look for *TGFBR2* mutations in 80 unrelated TAAD families, including the large family with disease linkage to 3p24–p25. Two *TGFBR2* mutations [c.1378C > T (p.R460C) and c.1379G > A (p.R460H)], both affecting the same amino acid residue in the serine/threonine kinase domain, were identified in four families, or approximately 5% of the TAAD cases (Pannu et al. 2005a) (Table 2, Fig. 1). Each mutation occurred in the unique haplotype block, indicating an independent mutation event.

The mutational hotspot at the p.R460 residue in TAAD2 suggested a positive phenotype–genotype correlation, and this observation was supported by the discovery of another family with p.R460H that was initially diagnosed as having TAAD2 and, later, as having a distinctive condition with cardiovascular findings consistent with TAAD2, together with arterious tortuosity and aneurysm (Law et al. 2005, 2006). Three additional missense *TGFBR2* mutations [c.1159G > A (p.V387G), c.1181G > A (p.C394Y), c.1657T > A (p.S553T)] and, more importantly, one *TGFBR1* mutation [c.1460G > A (p.R487Q)] were found in four TAAD patients (Matyas et al. 2006).

Shprintzen–Goldberg craniosynostosis syndrome

Shprintzen–Goldberg craniosynostosis syndrome (SGS, OMIM, #182212) is characterized by craniosynostosis and other craniofacial features, marfanoid skeletal abnormalities, and developmental delay (Robinson et al. 2005). Furlong syndrome (FS) is a similar marfanoid disorder with craniosynostosis, which differs from SGS by the absence of mental retardation (Furlong et al. 1987).

Table 2 Summary of *TGFBR2* and *TGFBR1* mutations

Gene	Disorder	Exon	Mutations	Domain	Splicing abnormality	Nature	Ghent criteria	References
TGFBR2	MFS	–	Chromosomal rearrangements	–	–	De novo	Fulfilled	Mizuguchi et al. (2004)
		4	c.923T > C (p.L308P)	Kinase	–	De novo	Fulfilled	Mizuguchi et al. (2004)
		4	c.1067G > C (p.R356P)	Kinase	–	De novo	Not fulfilled[a]	Sakai et al. (2006)
		4	c.1106G > T (p.G369V) and c.1159G > C (p.V387L)[b]	Kinase	–	Familial	Not fulfilled	Matyas et al. (2006)
		4	c.1151A > G (p.N384S)	Kinase	–	Familial	Not fulfilled	Singh et al. (2006)
		4	c.1188T > G (p.C396W) and c.-334T > A[c]	Kinase	–	De novo	Fulfilled	Singh et al. (2006)
		5	c.1273A > G (p.M425V)	Kinase	–	Familial	Fulfilled	Disabella et al. (2006)
		5	c.1336G > A (p.D446N)	Kinase	–	De novo	Not fulfilled	Disabella et al. (2006)
		5	c.1336G > A (p.D446N)	Kinase	–		Not fulfilled[a]	Sakai et al. (2006)
		5	c.1322C > T (p.S441F)	Kinase	–	De novo	Not fulfilled	Singh et al. (2006)
		5	c.1346C > T (p.S449F)	Kinase	–	Familial	Not fulfilled	Mizuguchi et al. (2004)
		5	c.1378C > T (p.R460C)	Kinase	–	Familial	Fulfilled	Singh et al. (2006)
		5	c.1379G > A (p.R460H)	Kinase	–	Familial	Fulfilled	Disabella et al. (2006)
		6	c.1489C > T (p.R497X)	Kinase	–	De novo?	Not fulfilled	Singh et al. (2006)
		6	c.1524G > A (p.Q508Q)	Kinase	+	Familial	Fulfilled	Mizuguchi et al. (2004)
		7	c.1561T > C (p.W521R)	Kinase	–	De novo	Fulfilled	Matyas et al. (2006)
		7	c.1609C > T (p.R537C)	Kinase	–	Familial	Fulfilled	Mizuguchi et al. (2004)
	LDS	–	IVS1-2A > G	–	+	De novo?	–	Loeys et al. (2005)
		4	c.773T > G (p.V258G)	Kinase	–	Familial	Fulfilled	Matyas et al. (2006)
		4	p.A329T	Kinase	–	?	–	Loeys et al. (2006)
		4	c.1006T > A (p.Y336N)	Kinase	–	Familial	–	Loeys et al. (2005)
		4	c.1063G > C (p.A355P)	Kinase	–	Familial	–	Loeys et al. (2005)
		4	c.1067G > C (p.R356P)	Kinase	–	De novo	–	Ki et al. (2005)
		4	c.1069G > T (p.G357W)	Kinase	–	De novo	–	Loeys et al. (2005)
		4	p.N384S	Kinase	–	?	–	Loeys et al. (2006)
		5	p.P427L	Kinase	–	?	–	Loeys et al. (2006)
		5	p.P427S	Kinase	–	?	–	Loeys et al. (2006)
		5	p.Y448H	Kinase	–	?	–	Loeys et al. (2006)
		5	p.S449F	Kinase	–	?	–	Loeys et al. (2006)
		5	p.M457K	Kinase	–	?	–	Loeys et al. (2006)
		5	p.R460H	Kinase	–	?	–	Loeys et al. (2006)
		5	p.C461Y	Kinase	–	?	–	Loeys et al. (2006)
		–	IVS5-1G > A		+	?	–	Loeys et al. (2006)
		6	p.R495X	Kinase	–	?	–	Loeys et al. (2006)
		7	p.E519K	Kinase	–	?	–	Loeys et al. (2006)
		7	p.C520Y	Kinase	–	?	–	Loeys et al. (2006)
		7	p.D524N	Kinase	–	?	–	Loeys et al. (2006)
		7	p.A527V	Kinase	–	?	–	Loeys et al. (2006)
		7	c.1582C > T (p.R528C)	Kinase	–	De novo	–	Loeys et al. (2005, 2006)
		7	c.1583G > A (p.R528H)	Kinase	–	De novo	–	Loeys et al. (2005, 2006)
		7	p.L529F	Kinase	–	?	–	Loeys et al. (2006)
		7	p.C533R	Kinase	–	?	–	Loeys et al. (2006)
		7	p.C533F	Kinase	–	?	–	Loeys et al. (2006)
		7	p.R537C	Kinase	–	?	–	Loeys et al. (2006)
		7	p.R537G	Kinase	–	?	–	Loeys et al. (2006)
	TAAD	4	c.1159G > A (p.V387M)	Kinase	–	Familial	–	Matyas et al. (2006)
		4	c.1181G > A (p.C394Y)	Kinase	–	?	–	Matyas et al. (2006)
		5	c.1378C > T (p.R460C)	Kinase	–	Familial	–	Pannu et al. (2005a)
		5	c.1379G > A (p.R460H)	Kinase	–	Familial	–	Pannu et al. (2005a) and Law et al. (2006)

Table 2 continued

Gene	Disorder	Exon	Mutations	Domain	Splicing abnormality	Nature	Ghent criteria	References
		7	c.1657T > A (p.S553T)	–	–	De novo?	–	Matyas et al. (2006)
	SGS (LDS?)	–	IVS5-2A > G	–	+	De novo	–	Kosaki et al. (2006)
TGFBR1	MFS	4	c.759G > A(p.M253I)	Kinase	–	Familial	Fulfilled	Singh et al. (2006)
		4	c.799A > C (p.N267H)	Kinase	–	Familial	Not fulfilled	Matyas et al. (2006)
		5	c.934G > A (p.G312S)	Kinase	–	Familial	Fulfilled	Singh et al. (2006)
		7	c.1135A > G (p.M379V)	Kinase	–	?	Not fulfilled	Sakai et al. (2006)
	LDS	4	c.599C > T (p.T200I)	GS	–	De novo	–	Loeys et al. (2005)
		4	p.K232E	Kinase	–	?	–	Loeys et al. (2006)
		4	p.F234L	Kinase	–	?	–	Loeys et al. (2006)
		4	c.722C > T (p.S241L)	Kinase	–	De novo	Fulfilled	Loeys et al. (2006) and Matyas et al. (2006)
		5	c.953T > G (p.M318R)	Kinase	–	De novo	–	Loeys et al. (2005)
		6	p.A350E	Kinase	–	?		Loeys et al. (2006)
		6	p.G353V	Kinase	–	?		Loeys et al. (2006)
		6	p.G374E	Kinase	–	?		Loeys et al. (2006)
		7	c.1199A > G (p.D400G)	Kinase	–	De novo	–	Loeys et al. (2005)
		9	p.N478S	Kinase	–	?		Loeys et al. (2006)
		9	c.1460G > C (p.R487P)	Kinase	–	Familial	–	Loeys et al. (2005, 2006)
		9	p.R487Q	Kinase	–	?		Loeys et al. (2006)
		9	p.R487W	Kinase	–	?		Loeys et al. (2006)
	TAAD	9	c.1460G > A (p.R487Q)	Kinase	–	De novo	–	Matyas et al. (2006)
	FS	4	c.722C > T (p.S241L)	Kinase	–	De novo	Fulfilled	Ades et al. (2006)

MFS Marfan syndrome, *LDS* Loeys-Dietz syndrome, *TAAD* Familial thoracic aortic aneurysms and dissections, *SGS* Shprintzen-Goldberg craniosynostosis syndrome, *FS* Furlong syndrome

[a] LDS facial features were recognized

[b] Two nucleotide changes in one allele

[c] Compound heterozygote

Although a question was raised on the involvement of *FBN1* abnormality in SGS (Robinson et al. 2005), at least two *FBN1* mutations were identified (Kosaki et al. 2006; Sood et al. 1996).

Furthermore, the initial study of five SGS patients failed to reveal mutations in either *TGFBR1* or *TGFBR2* (Loeys et al. 2005), but Kosaki et al. (2006) recently reported a *TGFBR2* mutation [IVS5-2A > G] (Table 2, Fig. 1) in an SGS patient with craniofacial and skeletal abnormalities, mild developmental delay, and cardiovascular features, including aortic regurgitation, annuloaortic ectasia and sigmoid configuration of the brachiocephalic, left common carotid and left subclavian arteries. Robinson et al. (2006), however, suggested that this patient might be more appropriately diagnosed as having LDS, due to the presence of bifid uvula and arterial manifestations.

An identical *TGFBR1* mutation [c.722C > T (p.S241L)] was reported in two unrelated patients described as having probable FS (Table 2, Fig. 1) (Ades et al. 2006). One of these patients had learning difficulties, and the other had normal intelligence (Ades et al. 2006). Systemic arterial tortuosity was not evaluated in either of them, but one showed bifid uvula, consistent with LDS. The same mutation was also reported in an LDS patient with hypertelorism, tortuous arteries and bifid uvula (Matyas et al. 2006).

Germline *TGFBR* mutations and connective tissue disorders

The various mutations, as well as gene disruption by chromosomal structural abnormality, suggest that loss-of-function mutations of *TGFBR2* are responsible for a wide spectrum of connective tissue disorders, but no simple genotype–phenotype correlation has been observed. It is intriguing that domain-specific germline mutations of *TGFB1* cause Camurati–Engelmann disease (CED, OMIM #131300) (Kinoshita et al. 2000) associated with marfanoid habitus, despite the absence of connective tissue fragility. *TGFB1* mutations in CED were shown to cause increased TGFβ signaling (Janssens et al. 2003). These findings suggest that abnormal TGFβ signaling could be responsible for the skeletal features of MFS. This hypothesis is corroborated by earlier studies describing the roles of TGFβ signaling in skeletal development (Alvarez and Serra 2004; Serra et al. 1999).

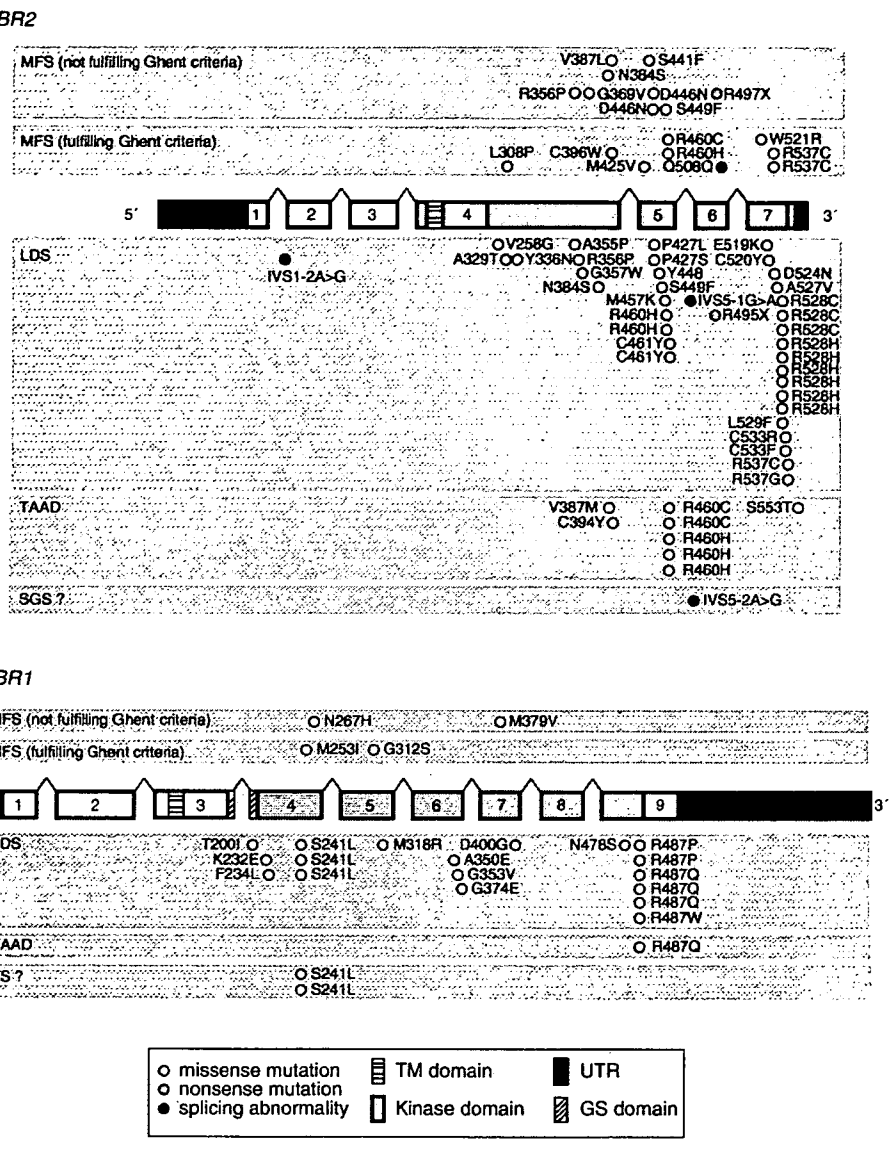

Fig. 1 Mutation spectrum of *TGFBR2* and *TGFBR1* identified in Marfan syndrome and its related disorders. *Numbered boxes* indicate exons of each gene. *Open and filled circles* represent missense and splicing abnormality mutations, respectively. Each mutation was found in a different family. Functional domains are shown as *patterned boxes*. *MFS* Marfan syndrome, *LDS* Loeys-Dietz syndrome, *TAAD* Familial thoracic aortic aneurysms and dissections, *SGS* Shprintzen-Goldberg craniosynostosis syndrome, *FS* Furlong syndrome

TGFBR2 and *TGFBR1* mutations found in MFS and its related disorders are generally associated with severe vascular consequences that differ somewhat from those found in patients with *FBN1* mutations. The vascular consequences associated with *TGFBR2* and *TGFBR1* mutations include aortic dissections in young age and aneurysms at sites distant from the aortic root. Thus, careful screening of arterial tortuosity and aneurysms from head to leg is highly recommended in this patient population.

Whether an MFS2 phenotype exists as a separate disorder from LDS is debatable. *TGFBR1* and *TGFBR2* aberrations are highly prevalent in LDS, which is characterized by severe cardiovascular features and family histories of aortic dissection with sudden death. Following the first report of *TGFBR2* mutations in MFS (Mizuguchi et al. 2004), LDS, TAAD2, SGS, and FS were recognized as *TGFBR* mutation-related disorders. Although the original MFS2 patients with *TGFBR2* mutations (Mizuguchi et al. 2004) could not be reasonably re-examined for the presence of LDS features such as bifid uvula, hypertelorism, craniosynostosis, and arterial tortuosity, at least three reports have since described *TGFBR1* or *TGFBR2* mutations in classic MFS patients in whom LDS had been ruled out (Disabella et al. 2006; Matyas et al. 2006; Singh et al. 2006). Four missense mutations [c.1273A > G (p.M425V), c.1378C > T (p.R460C), c.1379G > A (p.R460H), and c.1561T > C (p.W521R)] and compound heterozygous mutations [c.1337G > A (p.D446N) and c.-334T > A] in *TGFBR2* were identified in five patients with MFS that satisfied the Ghent

Table 3 Frequency of *TGFBR2/TGFBR1* mutations in MFS-related disorders

Diagnosis	FBN1 involvement	Gene tested	Mutations (%)		References
MFS	Negative	TGFBR2	25	(5/20)	Mizuguchi et al. (2004)
	Negative	TGFBR1	0	(0/7)	Loeys et al. (2005)
		TGFBR2	0	(0/7)	
	Negative	TGFBR2	100?	(3/3)[a]	Disabella et al. (2006)
	Negative or unknown	TGFBR2	3	(1/30)[b]	Ki et al. (2005)
	Negative	TGFBR1	5	(2/41)	Singh et al. (2006)
		TGFBR2	12	(5/41)	
	Negative	TGFBR1	5	(1/22)	Sakai et al. (2006)
		TGFBR2	9	(2/22)	
LDS	Unknown	TGFBR1	40	(4/10)	Loeys et al. (2005)
		TGFBR2	60	(6/10)	
	Unknown	TGFBR1	30	(9/30)	Loeys et al. (2006)
		TGFBR2	70	(21/30)	
LDS2	Unknown	TGFBR1	10	(4/40)	Loeys et al. (2006)
		TGFBR2	20	(8/40)	
TAAD	Unknown	TGFBR2	0	(0/10)	Mizuguchi et al. (2004)
	Unknown	TGFBR2	5	(4/80)	Pannu et al. (2005a)
SGS	Unknown	TGFBR1	0	(0/5)	Loeys et al. (2005)
		TGFBR2	0	(0/5)	
	Negative	TGFBR1	0	(0/1)	Kosaki et al. (2006)
		TGFBR2	100	(1/1)	
MD-CS/MR (FS)	Negative	TGFBR1	100	(2/2)[c]	Ades et al. (2006)
		TGFBR2	0	(0/2)	
MFS-related phenotypes	Negative	TGFBR1	4	(3/70)	Matyas et al. (2006)
		TGFBR2	9	(6/70)	

MFS Marfan syndrome, *LDS* Loeys-Dietz syndrome, *LDS2* Loeys-Dietz syndrome type II, *TAAD* Familial thoracic aortic aneurysms and dissections, *SGS* Shprintzen-Goldberg craniosynostosis syndrome, *MD-CS/MR* Marfan–craniosynostosis/mental retardation, *FS* Furlong syndrome

[a] Total number of patients screened was not described

[b] The patient was initially diagnosed as having an MFS variant, which was later refined as LDS

[c] The two patients with a *TGFBR1* mutation were categorized to Furlong syndrome

criteria. Seven more patients with MFS that did not satisfy the Ghent criteria were also reported to have mutations in *TGFBR2* (Disabella et al. 2006; Matyas et al. 2006; Sakai et al. 2006; Singh et al. 2006). In addition, two *TGFBR1* missense mutations [c.759G > A (p.M253I) and c.934G > A (p.G312S)] were found in two MFS patients and two *TGFBR1* mutations [c.799A > C (p.N267H) and c.1135A > G (p.M379V)] were identified in two patients not fulfilling MFS. Thus, *TGFBR2* and *TGFBR1* aberrations were observed in typical cases of classic MFS with no signs of LDS (Singh et al. 2006).

However, it should be noted that arterial tortuosity, a cardinal feature of LDS, was not systematically evaluated in any of the four studies (Disabella et al. 2006; Matyas et al. 2006; Sakai et al. 2006; Singh et al. 2006). Moreover, two research groups were unable to identify *TGFBR2* mutations in 29 MFS patients (*FBN1* was normal in 24 and unknown in five) (Ki et al. 2005) and seven patients (*FBN1* was normal) with MFS compatible with the Ghent criteria (Loeys et al. 2005). Thus, the question of whether an MFS2 phenotype and LDS should be classified as the same disorder remains unresolved.

At least six *TGFBR2* mutations (R356P, N384S, R460H, R460C, S449F, and R537C) and two *TGFBR1* mutations (S241L and R487Q) were recognized in two or three conditions (i.e., R460H found in MFS, LDS, and TAAD) (Ades et al. 2006; Disabella et al. 2006; Ki et al. 2005; Loeys et al. 2006; Matyas et al. 2006; Mizuguchi et al. 2004; Pannu et al. 2005a; Sakai et al. 2006; Singh et al. 2006) (Fig. 1, Table 2), implying that *TGFBR* mutations may cause various clinical consequences or that appropriate diagnosis is rather difficult for these disorders.

Pathogenesis of Marfan syndrome

Fibrillin-1 involvement in connective tissue disorders

Extracellular matrix (ECM) is formed by a number of macromolecules that are secreted and deposited into the space surrounding cells, where they are essential

for tissue development and homeostasis. Fibrillin-1 is an ECM protein that is assembled into microfibrillar networks, where it interacts with other ECM proteins. Fibrillin-rich microfibrils form peripheral components of elastic fibers, which play a role as an architectural foundation and provide elasticity to tissues (Kielty et al. 2002).

Fibrillin-1 is a multi-domain protein that contains three characteristic modules: an epidermal growth factor (EGF)-like motif, a latent TGFβ binding protein (LTBP) motif, and a fusion of the two (Fib motif). The majority of the EGF-like modules in the *FBN1* gene have a conserved calcium-binding sequence (cbEGF-like module).

Mutations associated with MFS are distributed over the entire *FBN1* gene. No genotype–phenotype correlation has been clearly established, except for neonatal MFS (nMFS). Most mutations causing nMFS seem to be clustered in exons 24–32, although other phenotypes are also associated with mutations in these exons.

The fibrillin-1 protein contains 47 EGF-like modules, characterized by six cysteine residues that form disulfide bonds with one another. Most MFS missense mutations occur in one of the 43 cbEGF-like modules (Boileau et al. 2005; Robinson and Godfrey 2000). These mutations are thought to influence the protein structure and calcium binding affinity of cbEGF-like modules, with various deleterious effects (Boileau et al. 2005; Downing et al. 1996).

In classical MFS the incidence of ectopia lentis was significantly higher in patients harboring cysteine substitutions in the cbEGF-like modules than in patients with premature termination codon (PTC) mutations (Arbustini et al. 2005; Biggin et al. 2004; Loeys et al. 2004; Rommel et al. 2005; Schrijver et al. 2002). Furthermore, isolated or predominant ectopia lentis is frequently associated with cysteine substitutions (Ades et al. 2004; Comeglio et al. 2002), suggesting that cysteine residues may have a critical function in suspensory ligaments of the eyes, as previously described (Rommel et al. 2005).

The dominant–negative mechanism of mutant fibrillin-1 in MFS pathology is an attractive hypothesis in the light of the polymerizing nature of fibrillin-1 molecules into microfibrils. Various studies have examined the correlation between the expression level of mutant mRNA produced by PTC mutations and the degree of clinical severity (Ades et al. 2004; Dietz et al. 1993; Schrijver et al. 2002). Nonsense-mediated mRNA decay could limit aberrant protein production from mutated alleles in heterozygous patients, but remnant mutant fibrillin-1 proteins may act in a dominant–negative fashion. However, the hypothesized association between expression level and clinical severity is controversial. It is also possible that different expression levels of normal *FBN1* alleles leads to different phenotypes in MFS family members sharing the same heterozygous PTC mutation (Hutchinson et al. 2003).

Support for the haploinsufficiency hypothesis as a mechanism in MFS pathogenesis comes from the finding of an *FBN1* deletion in a patient with a number of marfanoid characteristics (Hutchinson et al. 2003; Judge et al. 2004) as well as in mouse models (Judge et al. 2004). In transgenic mice carrying human mutant *FBN1* (p.C1663R), no obvious cardiovascular and skeletal signs have been recognized, despite the co-assembly of the mutant protein into mouse microfibrillar networks. Other knock-in mice (in which the p.C1039G mutation $Fbn1^{C1039G/+}$ targeted the endogenous *Fbn1*) showed decreased microfibrillar deposition, skeletal abnormalities and changes in the architecture of the aortic wall. Notably, the aortic wall phenotype was rescued by the wildtype *FBN1* transgene.

TGFβ signaling and connective tissue disorders

TGFβ is a secreted polypeptide that plays diverse roles in cell proliferation and differentiation, apoptosis, and extracellular matrix formation (Cohen 2003; Derynck et al. 2001; Ignotz and Massague 1986; Massague et al. 2000). TGFβ1 is abundant in the ECM. An inactive form of mature TGFβ1 stays in a complex with latency-associated polypeptide (LAP), which is an N-terminal peptide cleaved from proTGFβ1, and latent TGFβ binding protein (LTBP). Mature TGFβ1 and LAP are noncovalently associated in a small latency complex (SLC). The SLC binds to LTBP via disulfide bonds between LAP and LTBP, forming a large latency complex (LLC) (Annes et al. 2003). LTBP plays a role in folding and secreting TGFβ1, targeting it appropriately to the ECM, and modulating TGFβ activity (Charbonneau et al. 2004; Kaartinen and Warburton 2003; Ramirez et al. 2004; Rifkin 2005).

A recent study revealed that LTBP-1 (one of the LTBPs) and fibrillin interact in vitro and suggested that fibrillin-1 may stabilize the latent TGFβ complexes in the ECM (Isogai et al. 2003). Support for this hypothesis is seen in mouse models of MFS. Three strains of transgenic mice, each harboring a different type of *Fbn1* mutation, displayed several MFS features with variable severity (Judge et al. 2004; Pereira et al. 1997, 1999). Increased TGFβ activity was observed in at least four organs (lung, mitral valve, aortic and dural tissues), possibly as a result of excess free LLC due to inadequate stabilization within the ECM, as previously hypothesized (Habashi et al. 2006; Jones et al. 2005; Neptune

et al. 2003; Ng et al. 2004; Rifkin 2005). Administration of an anti-TGFβ neutralizing antibody rescued the lung, mitral valve, and aortic tissue phenotypes (Habashi et al. 2006; Neptune et al. 2003; Ng et al. 2004). Furthermore, aortic aneurysm was prevented by the administration of losartan, an angiotensin II type 1 receptor blocker that alleviates increased TGFβ activity (Habashi et al. 2006). Taken together, these findings support an association of abnormal TGFβ signaling with MFS pathogenesis. Interaction between the affected structural ECM components and aberrant TGFβ signaling may coordinately determine MFS phenotypes.

TGFβ transduces its signals via two distinct types of transmembrane receptors, type I (TβRI) and type II (TβRII), encoded by *TGFBR1* and *TGFBR2*, respectively (ten Dijke et al. 1996; Wrana et al. 1994). Both types of receptors consist of an extracellular domain, a transmembrane domain and a serine/threonine kinase domain. A glycine/serine-rich domain (GS domain) is specific for TβRI. The ligand-bound TβRII phosphorylates the GS domain, which then acts in signal transduction (Wieser et al. 1995).

It is likely that abnormal TGFβ signaling is involved in the human MFS phenotype. Identification of *TGFBR2* mutations in MFS2 supports the hypothesis and provided the first direct link between a human connective tissue disorder and abnormal TGFβ signaling. Loss-of-function *TGFBR2* mutations are hypothesized to cause MFS2, LDS and TAAD2. In our previous study mammalian cells were transfected with MFS2-related mutant *TGFBR2* constructs, and a luciferase assay clearly showed decreased TGFβ signaling activity (Mizuguchi et al. 2004). If the highly conserved p.R460 residue is essential for the structural integrity of the catalytic loop of TβRII, the p.R460 missense mutations found in TAAD2 could dramatically perturb TGFβ signaling (Pannu et al. 2005a).

By contrast, aortic tissues from LDS individuals showed increased TGFβ signaling activity. The heterozygous state (with one normal allele and the other mutant) of *TGFBR2* abnormality in affected individuals might not simply reflect a loss-of-function nature of the mutation, probably because of the complex regulation of the TGFβ signaling pathway (Loeys et al. 2005). Paradoxically, increased TGFβ signaling was also shown in the kinase-deficient TβRII transgenic mice (Denton et al. 2003).

Conclusion

Recent genetic studies of MFS, both in mice and humans, revealed that TGFβ signaling is involved in the pathogenesis of MFS and related disorders. *FBN1* abnormalities appear to be the major genetic cause of MFS, but not the only cause.

MFS-related disorders share many features with MFS. Clinical data should be carefully evaluated, with the recognition that incomplete data might lead to different diagnoses. Further studies are needed in order to establish frames of nosology for MFS and MFS-related disorders, by collection and analysis of extensive genetic and clinical data from many affected patients. An appropriate diagnostic system(s) is needed to differentiate MFS and MFS-related disorders.

Acknowledgment We thank Dr. Remco Visser at the Department of Pediatrics, Leiden University Medical Center, Leiden, The Netherlands, for his critical reading of this manuscript.

References

Ades LC, Holman KJ, Brett MS, Edwards MJ, Bennetts B (2004) Ectopia lentis phenotypes and the FBN1 gene. Am J Med Genet A 126:284–289

Ades LC, Sullivan K, Biggin A, Haan EA, Brett M, Holman KJ, Dixon J, Robertson S, Holmes AD, Rogers J, Bennetts B (2006) FBN1, TGFBR1, and the Marfan-craniosynostosis/mental retardation disorders revisited. Am J Med Genet A 140:1047–1058

Alvarez J, Serra R (2004) Unique and redundant roles of Smad3 in TGF-beta-mediated regulation of long bone development in organ culture. Dev Dyn 230:685–699

Annes JP, Munger JS, Rifkin DB (2003) Making sense of latent TGFbeta activation. J Cell Sci 116:217–224

Arbustini E, Grasso M, Ansaldi S, Malattia C, Pilotto A, Porcu E, Disabella E, Marziliano N, Pisani A, Lanzarini L, Mannarino S, Larizza D, Mosconi M, Antoniazzi E, Zoia MC, Meloni G, Magrassi L, Brega A, Bedeschi MF, Torrente I, Mari F, Tavazzi L (2005) Identification of sixty-two novel and twelve known FBN1 mutations in eighty-one unrelated probands with Marfan syndrome and other fibrillinopathies. Hum Mutat 26:494

Biggin A, Holman K, Brett M, Bennetts B, Ades L (2004) Detection of thirty novel FBN1 mutations in patients with Marfan syndrome or a related fibrillinopathy. Hum Mutat 23:99

Boileau C, Jondeau G, Babron MC, Coulon M, Alexandre JA, Sakai L, Melki J, Delorme G, Dubourg O, Bonaiti-Pellie C, et al (1993) Autosomal dominant Marfan-like connective-tissue disorder with aortic dilation and skeletal anomalies not linked to the fibrillin genes. Am J Hum Genet 53:46–54

Boileau C, Jondeau G, Mizuguchi T, Matsumoto N (2005) Molecular genetics of Marfan syndrome. Curr Opin Cardiol 20:194–200

Charbonneau NL, Ono RN, Corson GM, Keene DR, Sakai LY (2004) Fine tuning of growth factor signals depends on fibrillin microfibril networks. Birth Defects Res C Embryo Today 72:37–50

Cohen MM Jr (2003) TGF beta/Smad signaling system and its pathologic correlates. Am J Med Genet A 116:1–10

Collod G, Babron MC, Jondeau G, Coulon M, Weissenbach J, Dubourg O, Bourdarias JP, Bonaiti-Pellie C, Junien C, Boileau C (1994) A second locus for Marfan syndrome maps to chromosome 3p24.2-p25. Nat Genet 8:264–268

Collod-Beroud G, Le Bourdelles S, Ades L, Ala-Kokko L, Booms P, Boxer M, Child A, Comeglio P, De Paepe A, Hyland JC, Holman K, Kaitila I, Loeys B, Matyas G, Nuytinck L, Peltonen L, Rantamaki T, Robinson P, Steinmann B, Junien C, Beroud C, Boileau C (2003) Update of the UMD-FBN1 mutation database and creation of an FBN1 polymorphism database. Hum Mutat 22:199–208

Comeglio P, Evans AL, Brice G, Cooling RJ, Child AH (2002) Identification of FBN1 gene mutations in patients with ectopia lentis and marfanoid habitus. Br J Ophthalmol 86:1359–1362

Corson GM, Chalberg SC, Dietz HC, Charbonneau NL, Sakai LY (1993) Fibrillin binds calcium and is coded by cDNAs that reveal a multidomain structure and alternatively spliced exons at the 5′ end. Genomics 17:476–484

De Paepe A, Devereux RB, Dietz HC, Hennekam RC, Pyeritz RE (1996) Revised diagnostic criteria for the Marfan syndrome. Am J Med Genet 62:417–426

Denton CP, Zheng B, Evans LA, Shi-wen X, Ong VH, Fisher I, Lazaridis K, Abraham DJ, Black CM, de Crombrugghe B (2003) Fibroblast-specific expression of a kinase-deficient type II transforming growth factor beta (TGFbeta) receptor leads to paradoxical activation of TGFbeta signaling pathways with fibrosis in transgenic mice. J Biol Chem 278:25109–25119

Derynck R, Akhurst RJ, Balmain A (2001) TGF-beta signaling in tumor suppression and cancer progression. Nat Genet 29:117–129

Dietz HC, Cutting GR, Pyeritz RE, Maslen CL, Sakai LY, Corson GM, Puffenberger EG, Hamosh A, Nanthakumar EJ, Curristin SM, et al (1991) Marfan syndrome caused by a recurrent de novo missense mutation in the fibrillin gene. Nature 352:337–339

Dietz HC, McIntosh I, Sakai LY, Corson GM, Chalberg SC, Pyeritz RE, Francomano CA (1993) Four novel FBN1 mutations: significance for mutant transcript level and EGF-like domain calcium binding in the pathogenesis of Marfan syndrome. Genomics 17:468–475

Dietz H, Francke U, Furthmayr H, Francomano C, De Paepe A, Devereux R, Ramirez F, Pyeritz R (1995) The question of heterogeneity in Marfan syndrome. Nat Genet 9:228–229

Disabella E, Grasso M, Marziliano N, Ansaldi S, Lucchelli C, Porcu E, Tagliani M, Pilotto A, Diegoli M, Lanzarini L, Malattia C, Pelliccia A, Ficcadenti A, Gabrielli O, Arbustini E (2006) Two novel and one known mutation of the TGFBR2 gene in Marfan syndrome not associated with FBN1 gene defects. Eur J Hum Genet 14:34–38

Downing AK, Knott V, Werner JM, Cardy CM, Campbell ID, Handford PA (1996) Solution structure of a pair of calcium-binding epidermal growth factor-like domains: implications for the Marfan syndrome and other genetic disorders. Cell 85:597–605

Faivre L, Gorlin RJ, Wirtz MK, Godfrey M, Dagoneau N, Samples JR, Le Merrer M, Collod-Beroud G, Boileau C, Munnich A, Cormier-Daire V (2003) In frame fibrillin-1 gene deletion in autosomal dominant Weill–Marchesani syndrome. J Med Genet 40:34–36

Francke U, Berg MA, Tynan K, Brenn T, Liu W, Aoyama T, Gasner C, Miller DC, Furthmayr H (1995) A Gly1127Ser mutation in an EGF-like domain of the fibrillin-1 gene is a risk factor for ascending aortic aneurysm and dissection. Am J Hum Genet 56:1287–1296

Furlong J, Kurczynski TW, Hennessy JR (1987) New Marfanoid syndrome with craniosynostosis. Am J Med Genet 26:599–604

Gilchrist DM (1994) Marfan syndrome or Marfan-like connective-tissue disorder. Am J Hum Genet 54:553–554

Guo D, Hasham S, Kuang SQ, Vaughan CJ, Boerwinkle E, Chen H, Abuelo D, Dietz HC, Basson CT, Shete SS, Milewicz DM (2001) Familial thoracic aortic aneurysms and dissections: genetic heterogeneity with a major locus mapping to 5q13–14. Circulation 103:2461–2468

Habashi JP, Judge DP, Holm TM, Cohn RD, Loeys BL, Cooper TK, Myers L, Klein EC, Liu G, Calvi C, Podowski M, Neptune ER, Halushka MK, Bedja D, Gabrielson K, Rifkin DB, Carta L, Ramirez F, Huso DL, Dietz HC (2006) Losartan, an AT1 antagonist, prevents aortic aneurysm in a mouse model of Marfan syndrome. Science 312:117–121

Halliday DJ, Hutchinson S, Lonie L, Hurst JA, Firth H, Handford PA, Wordsworth P (2002) Twelve novel FBN1 mutations in Marfan syndrome and Marfan related phenotypes test the feasibility of FBN1 mutation testing in clinical practice. J Med Genet 39:589–593

Hasham SN, Willing MC, Guo DC, Muilenburg A, He R, Tran VT, Scherer SE, Shete SS, Milewicz DM (2003) Mapping a locus for familial thoracic aortic aneurysms and dissections (TAAD2) to 3p24–25. Circulation 107:3184–3190

Hutchinson S, Furger A, Halliday D, Judge DP, Jefferson A, Dietz HC, Firth H, Handford PA (2003) Allelic variation in normal human FBN1 expression in a family with Marfan syndrome: a potential modifier of phenotype? Hum Mol Genet 12:2269–2276

Ignotz RA, Massague J (1986) Transforming growth factor-beta stimulates the expression of fibronectin and collagen and their incorporation into the extracellular matrix. J Biol Chem 261:4337–4345

Isogai Z, Ono RN, Ushiro S, Keene DR, Chen Y, Mazzieri R, Charbonneau NL, Reinhardt DP, Rifkin DB, Sakai LY (2003) Latent transforming growth factor beta-binding protein 1 interacts with fibrillin and is a microfibril-associated protein. J Biol Chem 278:2750–2757

Janssens K, ten Dijke P, Ralston SH, Bergmann C, Van Hul W (2003) Transforming growth factor-beta 1 mutations in Camurati–Engelmann disease lead to increased signaling by altering either activation or secretion of the mutant protein. J Biol Chem 278:7718–7724

Jones KB, Myers L, Judge DP, Kirby PA, Dietz HC, Sponseller PD (2005) Toward an understanding of dural ectasia: a light microscopy study in a murine model of Marfan syndrome. Spine 30:291–293

Judge DP, Biery NJ, Keene DR, Geubtner J, Myers L, Huso DL, Sakai LY, Dietz HC (2004) Evidence for a critical contribution of haploinsufficiency in the complex pathogenesis of Marfan syndrome. J Clin Invest 114:172–181

Kaartinen V, Warburton D (2003) Fibrillin controls TGF-beta activation. Nat Genet 33:331–332

Kainulainen K, Karttunen L, Puhakka L, Sakai L, Peltonen L (1994) Mutations in the fibrillin gene responsible for dominant ectopia lentis and neonatal Marfan syndrome. Nat Genet 6:64–69

Katzke S, Booms P, Tiecke F, Palz M, Pletschacher A, Turkmen S, Neumann LM, Pregla R, Leitner C, Schramm C, Lorenz P, Hagemeier C, Fuchs J, Skovby F, Rosenberg T, Robinson PN (2002) TGGE screening of the entire FBN1 coding sequence in 126 individuals with Marfan syndrome and related fibrillinopathies. Hum Mutat 20:197–208

Ki CS, Jin DK, Chang SH, Kim JE, Kim JW, Park BK, Choi JH, Park IS, Yoo HW (2005) Identification of a novel TGFBR2 gene mutation in a Korean patient with Loeys–Dietz aortic aneurysm syndrome; no mutation in TGFBR2 gene in 30

patients with classic Marfan's syndrome. Clin Genet 68:561–563

Kielty CM, Sherratt MJ, Shuttleworth CA (2002) Elastic fibres. J Cell Sci 115:2817–2828

Kinoshita A, Saito T, Tomita H, Makita Y, Yoshida K, Ghadami M, Yamada K, Kondo S, Ikegawa S, Nishimura G, Fukushima Y, Nakagomi T, Saito H, Sugimoto T, Kamegaya M, Hisa K, Murray JC, Taniguchi N, Niikawa N, Yoshiura K (2000) Domain-specific mutations in TGFB1 result in Camurati–Engelmann disease. Nat Genet 26:19–20

Kosaki K, Takahashi D, Udaka T, Kosaki R, Matsumoto M, Ibe S, Isobe T, Tanaka Y, Takahashi T (2006) Molecular pathology of Shprintzen–Goldberg syndrome. Am J Med Genet A 140:104–108; author reply 109–110

Law C, Bunyan D, Castle B, Day L, Keeton B, Simpson I, Westwood G (2005) Clinical findings in a large family with a predisposition to aortic dilatation and dissection and an R460H mutation in TGFBR2. J Med Genet 42 [Suppl 1]:S31

Law CJ, Bunyan D, Castle B, Day L, Simpson I, Westwood G, Keeton B (2006) Clinical features in a family with a R460H mutation in TGFBR2. J Med Genet (in press)

Lee B, Godfrey M, Vitale E, Hori H, Mattei MG, Sarfarazi M, Tsipouras P, Ramirez F, Hollister DW (1991) Linkage of Marfan syndrome and a phenotypically related disorder to two different fibrillin genes. Nature 352:330–334

Loeys B, Nuytinck L, Delvaux I, De Bie S, De Paepe A (2001) Genotype and phenotype analysis of 171 patients referred for molecular study of the fibrillin-1 gene FBN1 because of suspected Marfan syndrome. Arch Intern Med 161:2447–2454

Loeys B, De Backer J, Van Acker P, Wettinck K, Pals G, Nuytinck L, Coucke P, De Paepe A (2004) Comprehensive molecular screening of the FBN1 gene favors locus homogeneity of classical Marfan syndrome. Hum Mutat 24:140–146

Loeys BL, Chen J, Neptune ER, Judge DP, Podowski M, Holm T, Meyers J, Leitch CC, Katsanis N, Sharifi N, Xu FL, Myers LA, Spevak PJ, Cameron DE, De Backer J, Hellemans J, Chen Y, Davis EC, Webb CL, Kress W, Coucke P, Rifkin DB, De Paepe AM, Dietz HC (2005) A syndrome of altered cardiovascular, craniofacial, neurocognitive and skeletal development caused by mutations in TGFBR1 or TGFBR2. Nat Genet 37:275–281

Loeys BL, Schwarze U, Holm T, Callewaert BL, Thomas GH, Pannu H, De Backer JF, Oswald GL, Symoens S, Manouvrier S, Roberts AE, Faravelli F, Greco MA, Pyeritz RE, Milewicz DM, Coucke PJ, Cameron DE, Braverman AC, Byers PH, De Paepe AM, Dietz HC (2006) Aneurysm syndromes caused by mutations in the TGF-beta receptor. N Engl J Med 355:788–798

Massague J, Blain SW, Lo RS (2000) TGFbeta signaling in growth control, cancer, and heritable disorders. Cell 103:295–309

Matyas G, Arnold E, Carrel T, Baumgartner D, Boileau C, Berer W, Steinmann B (2006) Identification and in silico analyses of novel TGFBR1 and TGFBR2 mutations in Marfan syndrome-related disorders. Hum Mutat 27:760–769

Milewicz DM, Michael K, Fisher N, Coselli JS, Markello T, Biddinger A (1996) Fibrillin-1 (FBN1) mutations in patients with thoracic aortic aneurysms. Circulation 94:2708–2711

Mizuguchi T, Collod-Beroud G, Akiyama T, Abifadel M, Harada N, Morisaki T, Allard D, Varret M, Claustres M, Morisaki H, Ihara M, Kinoshita A, Yoshiura K, Junien C, Kajii T, Jondeau G, Ohta T, Kishino T, Furukawa Y, Nakamura Y, Niikawa N, Boileau C, Matsumoto N (2004) Heterozygous TGFBR2 mutations in Marfan syndrome. Nat Genet 36:855–860

Neptune ER, Frischmeyer PA, Arking DE, Myers L, Bunton TE, Gayraud B, Ramirez F, Sakai LY, Dietz HC (2003) Dysregulation of TGF-beta activation contributes to pathogenesis in Marfan syndrome. Nat Genet 33:407–411

Ng CM, Cheng A, Myers LA, Martinez-Murillo F, Jie C, Bedja D, Gabrielson KL, Hausladen JM, Mecham RP, Judge DP, Dietz HC (2004) TGF-beta-dependent pathogenesis of mitral valve prolapse in a mouse model of Marfan syndrome. J Clin Invest 114:1586–1592

Pannu H, Fadulu VT, Chang J, Lafont A, Hasham SN, Sparks E, Giampietro PF, Zaleski C, Estrera AL, Safi HJ, Shete S, Willing MC, Raman CS, Milewicz DM (2005a) Mutations in transforming growth factor-beta receptor type II cause familial thoracic aortic aneurysms and dissections. Circulation 112:513–520

Pannu H, Tran-Fadulu V, Milewicz DM (2005b) Genetic basis of thoracic aortic aneurysms and aortic dissections. Am J Med Genet C Semin Med Genet 139:10–16

Pereira L, Andrikopoulos K, Tian J, Lee SY, Keene DR, Ono R, Reinhardt DP, Sakai LY, Biery NJ, Bunton T, Dietz HC, Ramirez F (1997) Targeting of the gene encoding fibrillin-1 recapitulates the vascular aspect of Marfan syndrome. Nat Genet 17:218–222

Pereira L, Lee SY, Gayraud B, Andrikopoulos K, Shapiro SD, Bunton T, Biery NJ, Dietz HC, Sakai LY, Ramirez F (1999) Pathogenetic sequence for aneurysm revealed in mice underexpressing fibrillin-1. Proc Natl Acad Sci U S A 96:3819–3823

Ramirez F, Sakai LY, Dietz HC, Rifkin DB (2004) Fibrillin microfibrils: multipurpose extracellular networks in organismal physiology. Physiol Genomics 19:151–154

Rifkin DB (2005) Latent transforming growth factor-beta (TGF-beta) binding proteins: orchestrators of TGF-beta availability. J Biol Chem 280:7409–7412

Robinson PN, Godfrey M (2000) The molecular genetics of Marfan syndrome and related microfibrillopathies. J Med Genet 37:9–25

Robinson PN, Neumann LM, Demuth S, Enders H, Jung U, Konig R, Mitulla B, Muller D, Muschke P, Pfeiffer L, Prager B, Somer M, Tinschert S (2005) Shprintzen–Goldberg syndrome: fourteen new patients and a clinical analysis. Am J Med Genet A 135:251–262

Robinson P, Neumann L, Tinschert S (2006) Response to Kosaki et al. "Molecular pathology of Shprintzen–Goldberg syndrome". Am J Med Genet 140A:109–110

Rommel K, Karck M, Haverich A, Schmidtke J, Arslan-Kirchner M (2002) Mutation screening of the fibrillin-1 (FBN1) gene in 76 unrelated patients with Marfan syndrome or Marfanoid features leads to the identification of 11 novel and three previously reported mutations. Hum Mutat 20:406–407

Rommel K, Karck M, Haverich A, von Kodolitsch Y, Rybczynski M, Muller G, Singh KK, Schmidtke J, Arslan-Kirchner M (2005) Identification of 29 novel and nine recurrent fibrillin-1 (FBN1) mutations and genotype–phenotype correlations in 76 patients with Marfan syndrome. Hum Mutat 26:529–539

Sakai H, Visser R, Ikegawa S, Ito E, Numabe H, Watanabe Y, Mikami H, Kondoh T, Kitoh H, Sugiyama R, Okamoto N, Ogata T, Fodde R, Mizuno S, Takamura K, Egashira M, Sasaki N, Watanabe S, Nishimaki S, Takada F, Nagai T, Okada Y, Aoka Y, Yasuda K, Iwasa M, Kogaki S, Harada N, Mizuguchi T, Matsumoto N (2006) Comprehensive genetic analysis of relevant four genes in 49 patients with

Marfan syndrome or Marfan-related phenotypes. Am J Med Genet A 140:1719–1725

Schrijver I, Liu W, Odom R, Brenn T, Oefner P, Furthmayr H, Francke U (2002) Premature termination mutations in FBN1: distinct effects on differential allelic expression and on protein and clinical phenotypes. Am J Hum Genet 71:223–237

Serra R, Karaplis A, Sohn P (1999) Parathyroid hormone-related peptide (PTHrP)-dependent and -independent effects of transforming growth factor beta (TGF-beta) on endochondral bone formation. J Cell Biol 145:783–794

Singh KK, Rommel K, Mishra A, Karck M, Haverich A, Schmidtke J, Arslan-Kirchner M (2006) TGFBR1 and TGFBR2 mutations in patients with features of Marfan syndrome and Loeys–Dietz syndrome. Hum Mutat 27: 770–777

Sood S, Eldadah ZA, Krause WL, McIntosh I, Dietz HC (1996) Mutation in fibrillin-1 and the Marfanoid-craniosynostosis (Shprintzen–Goldberg) syndrome. Nat Genet 12:209–211

ten Dijke P, Miyazono K, Heldin CH (1996) Signaling via hetero-oligomeric complexes of type I and type II serine/threonine kinase receptors. Curr Opin Cell Biol 8:139–145

Tynan K, Comeau K, Pearson M, Wilgenbus P, Levitt D, Gasner C, Berg MA, Miller DC, Francke U (1993) Mutation screening of complete fibrillin-1 coding sequence: report of five new mutations, including two in 8-cysteine domains. Hum Mol Genet 2:1813–1821

Vaughan CJ, Casey M, He J, Veugelers M, Henderson K, Guo D, Campagna R, Roman MJ, Milewicz DM, Devereux RB, Basson CT (2001) Identification of a chromosome 11q23.2–q24 locus for familial aortic aneurysm disease, a genetically heterogeneous disorder. Circulation 103:2469–2475

Wieser R, Wrana JL, Massague J (1995) GS domain mutations that constitutively activate T beta R-I, the downstream signaling component in the TGF-beta receptor complex. EMBO J 14:2199–2208

Wrana JL, Attisano L, Wieser R, Ventura F, Massague J (1994) Mechanism of activation of the TGF-beta receptor. Nature 370:341–347

MOLECULAR AND CELLULAR BIOLOGY, Jan. 2007, p. 732–742 Vol. 27, No. 2
0270-7306/07/$08.00+0 doi:10.1128/MCB.01329-06

Role of DNA Methylation and Histone H3 Lysine 27 Methylation in Tissue-Specific Imprinting of Mouse *Grb10*[▽]

Yoko Yamasaki-Ishizaki,[1,2,8] Tomohiko Kayashima,[1] Christophe K. Mapendano,[1] Hidenobu Soejima,[3] Tohru Ohta,[4,8] Hideaki Masuzaki,[2] Akira Kinoshita,[1,8] Takeshi Urano,[5] Ko-ichiro Yoshiura,[1,8] Naomichi Matsumoto,[6] Tadayuki Ishimaru,[2] Tsunehiro Mukai,[3] Norio Niikawa,[1,8] and Tatsuya Kishino[7,8]*

Departments of Human Genetics[1] and Obstetrics and Gynecology,[2] Graduate School of Biomedical Sciences, Nagasaki University, Nagasaki, Japan; Department of Biomolecular Sciences, Saga University, Saga, Japan[3]; The Research Institute of Personalized Health Sciences, Health Sciences University of Hokkaido, Hokkaido, Japan[4]; Department of Biochemistry II, Graduate School of Medicine, Nagoya University, Nagoya, Japan[5]; Department of Human Genetics, Graduate School of Medicine, Yokohama City University, Yokohama, Japan[6]; Division of Functional Genomics, Center for Frontier Life Sciences, Nagasaki University, Nagasaki, Japan[7]; and CREST, Japan Science and Technology Agency, Kawaguchi, Japan[8]

Received 19 July 2006/Accepted 24 October 2006

Mouse *Grb10* is a tissue-specific imprinted gene with promoter-specific expression. In most tissues, *Grb10* is expressed exclusively from the major-type promoter of the maternal allele, whereas in the brain, it is expressed predominantly from the brain type promoter of the paternal allele. Such reciprocally imprinted expression in the brain and other tissues is thought to be regulated by DNA methylation and the Polycomb group (PcG) protein Eed. To investigate how DNA methylation and chromatin remodeling by PcG proteins coordinate tissue-specific imprinting of *Grb10*, we analyzed epigenetic modifications associated with *Grb10* expression in cultured brain cells. Reverse transcriptase PCR analysis revealed that the imprinted paternal expression of *Grb10* in the brain implied neuron-specific and developmental stage-specific expression from the paternal brain type promoter, whereas in glial cells and fibroblasts, *Grb10* was reciprocally expressed from the maternal major-type promoter. The cell-specific imprinted expression was not directly related to allele-specific DNA methylation in the promoters because the major-type promoter remained biallelically hypomethylated regardless of its activity, whereas gametic DNA methylation in the brain type promoter was maintained during differentiation. Histone modification analysis showed that allelic methylation of histone H3 lysine 4 and H3 lysine 9 were associated with gametic DNA methylation in the brain type promoter, whereas that of H3 lysine 27 regulated by the Eed PcG complex was detected in the paternal major-type promoter, corresponding to its allele-specific silencing. Here, we propose a molecular model that gametic DNA methylation and chromatin remodeling by PcG proteins during cell differentiation cause tissue-specific imprinting in embryonic tissues.

Genomic imprinting in mammals describes the situation where there is nonequivalence in expression between the maternal and paternal alleles at certain gene loci, depending on the parental origin. Genomic imprinting plays essential roles in development, growth, and behavior (6, 30, 31). Such parental origin-specific gene regulation is caused by epigenetic modifications that occur during gametogenesis without any nucleic acid changes. One of the well-known epigenetic modifications is DNA methylation. In the imprinted loci, differentially methylated regions between the maternal and paternal alleles are often found and associated with parental allele-specific expression (7). Another well-known epigenetic modification is histone modification, which represents the determinant of epigenetic features associated with imprinted genes. It has been reported that parental origin-specific gene expression on some imprinted genes is determined by DNA methylation and/or histone modifications (12, 13, 16, 23, 29, 40). Polycomb group (PcG) proteins also play an important role in various epigenetic phenomena (3), such as maintaining the silent state of the homeotic genes, maintaining X-chromosome inactivation (36), and silencing imprinted genes in mammals (24, 33). PcG protein complexes are thought to maintain long-term gene silencing during development through alterations of local chromatin structure (3, 27).

Mouse *Grb10* encoding the growth factor receptor-bound protein 10 (Grb10) is an imprinted gene with tissue-specific and promoter-specific expression. In most tissues, the major-type transcript of *Grb10* is expressed exclusively from the major-type promoter of the maternal allele, whereas in the brain, the brain type transcript is expressed predominantly from the brain type promoter of the paternal allele (1, 17). DNA methylation analysis has revealed that the CpG island (CGI) in the brain type promoter (CGI2) was gametically methylated in the oocyte as a primary imprint and remained methylated exclusively on the maternal allele in somatic tissues, while the CpG island in the major-type promoter (CGI1) was biallelically hypomethylated in somatic tissues (see Fig. 1 and 4) (17). Hikichi et al. proposed the model for tissue-specific imprinting of *Grb10* that the major-type transcript is regulated by DNA methylation-sensitive insulator (CTCF) binding in CGI2 and

* Corresponding author. Mailing address: Division of Functional Genomics, Center for Frontier Life Sciences, Nagasaki University, Sakamoto 1-12-4, Nagasaki 852-8523, Japan. Phone: 81-95-849-7120. Fax: 81-95-849-7178. E-mail: kishino@net.nagasaki-u.ac.jp.

▽ Published ahead of print on 13 November 2006.

the brain type transcript is regulated by putative brain-specific activators (17). They suggested that allelic DNA methylation in CGI2 can orchestrate reciprocal imprinting of the two promoters of the *Grb10* gene. This model was partially supported by the imprinting analysis of knockout mice of the *Dnmt3L* gene, encoding a factor for acquisition of maternal methylation imprint in germ cells (14, 18). In the embryos (*Dnmt3L*$^{m-/-}$), produced from *Dnmt3L*$^{-/-}$ females, maternal chromosome-specific DNA methylation in CGI2 was lost and null expression of the major-type transcript was detected (2). Recently, the PcG protein Eed (embryonic ectoderm development) was identified as a member of a new class of *trans*-acting factors, which regulate the expression of some paternally repressed imprinted genes, *Cdkn1c*, *Ascl2*, *Meg3*, and *Grb10* (24). In *Eed*$^{-/-}$ embryos, the major-type transcript of *Grb10* was biallelically expressed from the major-type promoter without major alteration of DNA methylation in gametically methylated CGI2, albeit various hypomethylated patterns were observed on the paternal allele (24). The expression analysis of these knockout mice suggests that DNA methylation and chromatin remodeling by PcG proteins represent the epigenetic factors that are necessary for establishing and/or maintaining the imprinted expression of *Grb10*. It remains unknown how they coordinate the tissue-specific and promoter-specific imprinting of *Grb10*.

Recently, mouse genes with brain-specific imprinting patterns were reported. They are *Ube3a* and *Murr1*, with neuron-specific and brain developmental stage-specific expressions, respectively. *Ube3a* is biallelically expressed in most tissues but expressed exclusively from the maternal allele only in neurons, leading to apparent partial imprinting with predominant maternal *Ube3a* expression in the whole brain (38). *Murr1* is imprinted in the adult brain, especially in mature neurons, but not in embryonic and neonatal brains (37). These lines of evidence suggest that brain-specific imprinting may be regulated in part by epigenetic modifications, depending on specification and maturation of cell lineages in the developing brain (9, 19).

Since *Grb10* is a tissue-specific imprinted gene, we hypothesized that tissue-specific reciprocal imprinting of *Grb10* also depends on cell-specific epigenetic modifications acquired during cell differentiation. To examine our hypothesis, we performed an epigenetic analysis of brain cells with the aid of primary cortical cell cultures, in which neurons or glial cells were cultured separately from products of reciprocal crosses between the C57BL/6 and PWK strains (divergent strains of *Mus musculus*). In each cultured brain cell, *Grb10* expression and epigenetic factors such as DNA methylation and histone modifications were analyzed to investigate how DNA methylation and chromatin remodeling by PcG proteins establish and maintain the tissue-specific and promoter-specific imprinting of *Grb10*.

MATERIALS AND METHODS

Mice. All procedures were performed with approval from the Nagasaki University Institutional Animal Care and Use Committee. F_1 hybrid mice were obtained by mating C57BL/6 females with PWK males [(C57BL/6 × PWK)F_1] and vice versa [(PWK × C57BL/6)F_1]. Telencephalon/cerebral cortices and embryonic fibroblasts were prepared from embryonic day 10 (E10) to E15. Tissues were used for RNA and DNA extraction or primary cultures. Brain tissue for reverse transcriptase (RT) PCR was dissected at E10, E16, postnatal day 1, postnatal day 5, 2 weeks, 4 weeks, 6 weeks, and 14 months.

Primary culture. Methods of primary cultures of cortical neurons, glial cells, and embryonic fibroblasts have been described elsewhere (38). In brief, E15 cerebral cortices without meninges were trypsinized to dissociate brain cells. For neuronal culture, dissociated cells were cultured in neurobasal medium (Gibco BRL, Carlsbad, CA) with B27 supplement (Gibco BRL). Cultures were maintained in 5% CO_2 at 37°C for 5 days. For the long culture, half of the culture medium was changed every 3 to 4 days. For glial cell culture, dissociated brain cells were cultured overnight in Dulbecco's modified Eagle's medium (Sigma, St. Louis, MO) supplemented with 10% fetal calf serum, and then the medium was changed to Neurobasal medium (Gibco BRL) with G5 supplement (GIBCO BRL). After 5 to 7 days in the primary culture, cultured glial components were subcultured. Cultures were maintained in 5% CO_2 at 37°C for a total of 14 days. For embryonic fibroblast culture, embryonic fibroblasts derived from E15 embryonic skin were cultured in Dulbecco's modified Eagle's medium supplemented with 10% fetal calf serum.

cDNA synthesis. Total RNA was isolated from cultured cells and tissues with RNeasy (QIAGEN, Hilden, Germany) according to the manufacturer's protocol. The RNA was treated with amplification grade DNase I (Invitrogen, Carlsbad, CA) to degrade any genomic DNA present in the sample. The cDNA was generated from total RNA by SuperScript II reverse transcriptase (Invitrogen) primed with oligo(dT)$_{12-18}$ primers. The first-strand cDNA was synthesized at 42°C for 50 min. Then, mRNA-cDNA chains were denatured and the reverse transcriptase activity was arrested by heating at 70°C for 15 min. An identical reaction was carried out without reverse transcriptase as a negative control.

RT-PCR for expression analysis. The cDNA obtained was used to perform RT-PCR for expression analysis. The expression of each *Grb10* transcript was analyzed using primers 1aF and 1R for the major-type transcript and using primers 1bF and 1R for the brain type transcript. Other transcripts, including exon 1c, were amplified by primer sets 1cF/e2R and 1aF/1cR. PCR amplification with primers 1aF and 1R was performed for 32 to 35 cycles of 15 s at 96°C, 20 s at 60°C, and 60 s at 72°C, with primers 1bF and 1R for 32 to 38 cycles of 15 s at 96°C, 20 s at 60°C, and 60 s at 72°C, and with primer sets 1cF/e2R and 1aF/1cR for 35 cycles of 15 s at 96°C, 20 s at 60°C, and 60 s at 72°C. The primers for *Map2*, *Gfap*, and *Gapdh* used for evaluation of the cultured cells have been described elsewhere (38). For a semiquantitative RT-PCR, optimal template cDNA concentrations were determined according to *Gapdh* amplification. PCR products were amplified for 25 to 30 cycles of 15 s at 96°C, 20 s at 55°C, and 30 s at 72°C.

Quantitative analysis of gene expression by real-time PCR. cDNA was applied to real-time PCR for quantitative analysis of each transcript using SYBR green and an ABI Prism 7900 (PE Applied Biosystems, Foster City, CA). PCR was performed on samples at least in triplicate according to the manufacturer's protocol to control for PCR variation. To standardize each experiment, the results were represented as a percentage of expression, calculated by dividing the average value of the expression of the target gene by that of an internal control gene, *Gapdh* (38). The primers used for real-time PCR were primers 1aF and1R for the major-type transcript and primers Q-1bF and Q-1bR for the brain type transcript. Each experiment was repeated with independent RNAs two to three times.

Sequencing for allelic differences. A sequence chromatogram was used to detect allelic differences of PCR products. Parental expression of major/brain type transcripts in the brain and kidney was analyzed by RT-PCR using primer sets 1aF/coR and 1bF/coR for 35 to 38 cycles of 15 s at 96°C, 20 s at 60°C, and 120 s at 72°C. Parental chromosome-specific histone modifications in the major-type promoter were analyzed by PCR using the primer set ChIP-F/ChIP-R for 30 cycles of 30 s at 95°C, 30 s at 58°C, and 30 s at 72°C. The PCR products were analyzed by direct sequencing with a BigDye Terminator cycle sequencing kit (PE Applied Biosystems) on an automated sequencer, the ABI Prism 3100 genetic analyzer (PE Applied Biosystems).

DNA methylation analysis. Isolated DNA was treated with sodium bisulfite using a CpGenome DNA modification kit (Chemicon International Inc., Temecula, CA) according to the manufacturer's protocol. Bisulfite-treated DNA samples were subjected to nested PCR amplification using the following first and second primer pairs, respectively, for each CGI; CGI1, Me1F/Me-1R and Me-1F'/Me-1R'; CGI2, Me-2F/Me-2R and Me-2F'/Me-2R'; and CGI3, Me-3F/Me-3R and Me-3F'/Me-3R'. After the first PCR using the first primer set, the products were used as templates for nested PCR using the second primer set. The nested PCR products were cloned into the TA cloning vector (Invitrogen), and at least 32 clones for each sample were sequenced.

ChIP. A chromatin immunoprecipitation (ChIP) assay was performed with a ChIP assay kit (Upstate Biotechnology, Lake Placid, NY) according to the manufacturer's protocol. In brief, the chromatin of cultured cells was prepared from ~1.0 × 10^6 cells and treated with formaldehyde to cross-link DNA to

TABLE 1. Primers used in this study

Function(s) and primer	Sequence (5′–3′)	Annealing temp (°C) (PCR cycle no.)[a]
Expression and imprinting analysis		
1aF[b]	CACGAAGTTTCCGCGCA	
1bF	GCGATCATTCGTCTCTGAGC	
1R[b]	AGTATCAGTATCAGACTGCATGTTG	
1cF	ATCGCCATCTACAGTTTCTG	
1cR	CAAGGTACAGAGCTAGGACG	
e2R	CTGGTTGGCTTCTTTGTTGTGG	
coR	TACGGATCTGCTCATCTTCG	
ChIP-F	TCACTTTAGAAACCGGGCA	
ChIP-R	AAACTCGGGCTTGCTCA	
Quantitative analysis		
Q-1bF	TCATTCGTCTCTGAGCGGCA	
Q-1bR	ATACGTGTTACATGCGCCAA	
Q-ChIP1F	TCACTTTAGAAACCGGGCA	
Q-ChIP1R	AAACTCGGGCTTGCTCA	
Q-ChIP2F	GATCATTCGTCTCTGAGC	
Q-ChIP2R	ATGCGGCAACATGCGCTGACA	
Hot-stop PCR and SSCP analysis		
ChIP2F-1	TCATTCGTCTCTGAGCGGCA	60 (32)
ChIP2R-1	TCTGGAGCCTAGAGGAGCG	
ChIP2F-2	AAGCGCGTGCTGGTTTGTA	60 (35)
ChIP2R-2	ATACGTGTTACATGCGCCAA	
DNA methylation analysis		
CGI1 1st		53 (35)
Me-1F	TGGGGTTTAATATTAAGTTTGA	
Me-1R	TTACATCTCTTAAATAAAACA	
CGI1 2nd		53 (35)
Me-1F′	TGGGGTTTAATATTAAGTTTGA	
Me-1R′	AAATCACCTATAACTCTCCTAC	
CGI2 1st		50 (40)
Me-2F	TGGAGTTTAGAGGAG	
Me-2R	AATAGTTATTTTAGTAAGGG	
CGI2 2nd		50 (10)
Me-2F′	TGGAGTTTAGAGGAG	
Me-2R′	TAAGTGAAGTAATATAGTT	
CGI3 1st		53 (40)
Me-3F	AAAGAAGGTTTGGAGAGATTATTT	
Me-3R	CAAACCAAAACTTACTATATTTAATTTAAAC	
CGI3 2nd		53 (10)
Me-3F′	AAGGTTTGGAGAGATTATTTTTGATT	
Me-3R′	TAATTTAAACTTAACACTATTAAATACC	

[a] For expression and imprinting analysis, the annealing temperature and PCR cycle number depend on the combination of primers used for each analysis. See details in Materials and Methods. For quantitative analysis, the PCR conditions were decided according to the manufacturer's protocol.
[b] Also used for quantitative analysis.

protein in situ, sonicated to an average size of 0.5 kb, and immunoprecipitated with antibodies. Antibodies against acetyl histone H3 (H3Ac; catalog no. 06-599), acetyl histone H4 (H4Ac; catalog no. 09-866), Lys4 dimethylated histone H3 (H3mK4; catalog no. 07-030), Lys9 trimethylated H3 (H3me3K9; catalog no. 07-212), and Lys27 trimethylated H3 (H3mK27; catalog no. 07-449) were obtained from Upstate Biotechnology. The monoclonal antibody against Lys9 dimethylated histone H3 (H3me2K9) was developed previously (26). Immunoprecipitated samples without antibodies or with rabbit immunoglobulin G precipitation were used as negative controls for precipitations with specific antibodies in each experiment.

Quantitative analysis of immunoprecipitated DNA by real-time PCR. Immunoprecipitated DNA and input DNA were analyzed by real-time PCR using the same protocol as that used for gene expression analysis. For DNA immunoprecipitated with H3Ac, H4Ac, and H3mK4 antibodies, the quantitative value of immunoprecipitated DNA in each CGI was normalized by dividing the average value of each CGI by that of the internal control, *Gapdh*. For DNA immunoprecipitated with H3me2K9 and H3me3K9 antibodies, the average value of *D13Mit55* was used instead of the value of *Gapdh*. Each normalized value of immunoprecipitated DNA was further divided by the normalized value of the corresponding input DNA. For the evaluation of DNA immunoprecipitated with H3mK27 antibody, the results were presented as a percentage of immunoprecipitation, calculated by dividing the average value of immunoprecipitated DNA by the average value of the corresponding input DNA. Each experiment was performed three times with independent chromatin extracts. The primers used for real-time PCR were primers Q-ChIP1F and Q-ChIP1R for CGI1 analysis and primers Q-ChIP2F and Q-ChIP2R for CGI2 analysis. The primers for *Gapdh* and *D13Mit55* have been described elsewhere (16).

Hot-stop PCR and SSCP analysis. Hot-stop PCR was performed for the analysis of allele-specific histone modifications as follows. After a number of PCR cycles sufficient to detect a product using primers ChIP2F-1 and ChIP2R-1, primer ChIP2R-1 labeled by [γ-^{32}P]ATP was added to the mixture, and then one cycle of PCR was performed. The PCR products were digested with the restriction endonuclease Hpy188I and electrophoresed in a 4% polyacrylamide gel. Single-strand conformation polymorphism (SSCP) analysis of PCR products was performed for allele-specific histone methylation in the presence of [γ-^{32}P]ATP-labeled primers ChIP2F-2 and ChIP2R-2. PCR products were resolved by electrophoresis in an MDE nondenaturing acrylamide gel (FMC BioProduct, Rockland, ME).

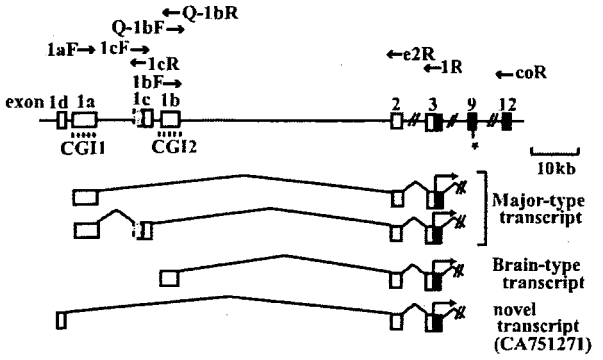

FIG. 1. Tissue-specific transcripts of *Grb10*. Filled boxes, open boxes, and shaded boxes represent protein-coding regions, 5′ untranslated regions, and extended exons 1c, respectively. The dashed lines indicate the CpG islands (CGI1 and CGI2) in the promoters. The primers used for RT-PCR are shown. The asterisk indicates the polymorphic site (G/A) between the C57BL/6 and PWK strains.

Primers. The primers used for the analysis are listed in Table 1.

RESULTS

Mouse *Grb10* has several tissue-specific promoters. Three different promoters of *Grb10* have previously been reported to initiate tissue-specific transcripts (Fig. 1). We first analyzed the expression of each transcript in E16 fetal tissues. The major-type transcript amplified by PCR using primers 1aF and e2R in exons 1a and 2, respectively, was detected in the fetal brain but was less detected in other tissues, while the brain type transcript amplified by primers 1bF and e2R in exons 1b and 2, respectively, was detected exclusively in the fetal brain (Fig. 2A). Another transcript which was previously reported to be brain specific in adult tissues (1) was examined in fetal tissues. PCR using primers 1cF and e2R in exons 1c and 2, respectively, showed that exon 1c was expressed not only in the fetal brain but also in the fetal liver and kidney (Fig. 2A). To assess whether exon 1c is an alternatively spliced exon of the major-type transcript with exon 1a, we performed PCR using primers 1aF and 1cR in exons 1a and 1c, respectively. The PCR product containing exons 1a and 1c was detected in the fetal tissues (Fig. 2A). Sequence analysis of the RT-PCR product revealed that exon 1c was extended 67 bp upstream of the previously published exon 1c with the consensus splicing site (Fig. 1). Any RT-PCR products with both exons 1a and 1b or both exons 1c and 1b were not found (data not shown). Furthermore, we identified another putative exon, 1d, located 1.2 kb upstream of exon 1a in the expressed sequence tag database (GenBank accession no. CA751271). The existence of the novel exon 1d was confirmed by RT-PCR in the embryonic liver but not in other tissues, including the brain (data not shown).

Expression of *Grb10* shifts from the major-type to the brain type transcript during brain development. To confirm whether the expression level of the brain type transcript changes during brain development, the major-type and brain type transcripts arising from exons 1a and 1b, respectively, were quantitatively analyzed at various developmental stages of the brain. Real-time PCR analysis showed that in the brain, the major-type transcript was highly expressed at E10 and decreased according to brain development, while expression of the brain type transcript was high in the perinatal period and gradually decreased thereafter (Fig. 2B). The result indicates that *Grb10* transcripts shift from the major type to the brain type during early brain development.

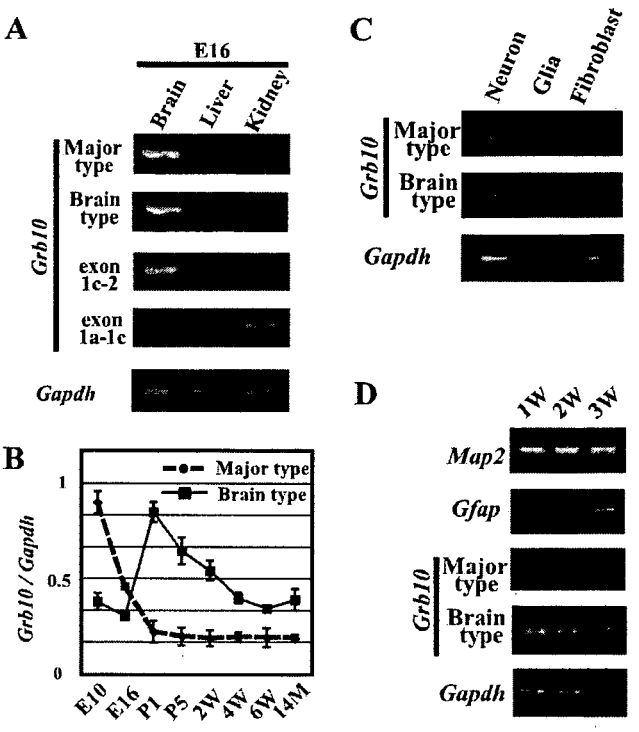

FIG. 2. Expression analysis of each transcript in embryonic tissues by RT-PCR. (A) Semiquantitative analysis of tissues from the E16 embryo. Exon 1c-2 and exon 1a-1c represent RT-PCR products amplified by primer sets 1cF/e2R and 1aF/1cR, respectively. The concentration of each cDNA was adjusted for *Gapdh* amplification as an internal control. (B) Quantitative evaluation of major-type and brain type transcripts in brain tissues from different developmental stages by real-time PCR. The relative amounts of major-type and brain type transcripts are shown. The relative amount of each transcript was calculated by normalizing each value with an internal control, *Gapdh*. Standard errors of the means are indicated by bars. (C) Expression analysis of major-type and brain type transcripts in the primary cell culture. (D) Evaluation of expression of marker genes and each *Grb10* transcript according to the culture period. 1w (1 week), 2w (2 weeks), and 3w (3 weeks) indicate the periods of neuron culture. P1, postnatal day 1; 14M, 14 months.

The brain-specific transcript is expressed in neurons but not in glial cells. Is the brain type transcript expressed exclusively in the brain restricted to the cell type? To know which type of brain cells, neurons or glial cells, express the brain type transcript, expression analysis of cultured neurons and glial cells was carried out. Prior to the analysis, we confirmed by immunostaining and RT-PCR with the brain precursors, neuronal and glial markers, that over 95% of the two cultured cell types were postmitotic neurons and astrocytes, respectively (data not shown). RT-PCR in cultured cells revealed that the major-type transcript was expressed in all cultured brain cells but that the brain type transcript was expressed only in neurons (Fig. 2C). We next tried to investigate whether these transcripts in the brain were associated with the maturation of

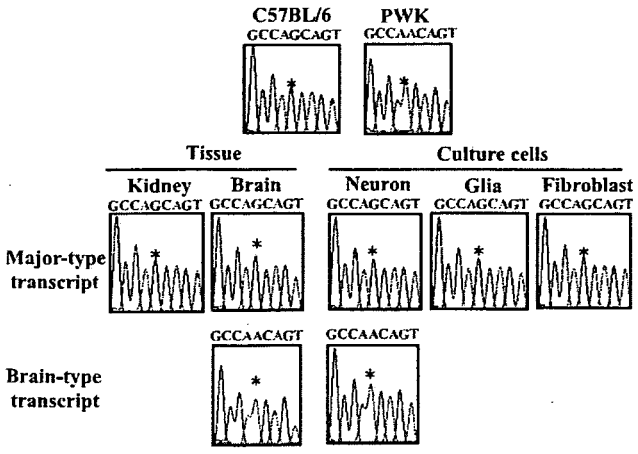

FIG. 3. Imprinting analysis of promoter-specific expression of *Grb10* by sequence chromatograms. Upper panels show the chromatograms of the genomic PCR products from each strain. Middle and lower panels show the chromatograms of the RT-PCR products from tissues and cultured cells of the F_1 hybrid, in which alleles were distinguished by the single-nucleotide (G/A) polymorphism (*) at exon 9.

neurons. Neurons were cultured for 1, 2, and 3 weeks, and semiquantitative RT-PCR was carried out. Before expression analysis of *Grb10*, the status of cell proliferation and differentiation by long culture was evaluated by primers for *Map2* as a marker for neurons and *Gfap* as a marker for astrocytes under the normalization of cDNA concentration to *Gapdh* (Fig. 2D). The expression of *Map2* never changed in 3-week-cultured cells, while that of *Gfap* was detected in the cells cultured for 3 weeks. In these long-culture cells, the brain type transcript was continuously expressed during culture periods, while the major-type transcript was less expressed than the brain type transcript. These results suggest that both types of transcripts are expressed in neurons and that the switching of the promoter from the major type to the brain type is observed during long culture periods.

Promoter-specific paternal expression of *Grb10* in the brain. To investigate the imprinted expression of *Grb10*, we first examined parental expression of the major-type and the brain type transcripts in the brain and kidney from F_1 hybrid mice by direct sequencing of the RT-PCR product. A polymorphic site (G/A) in exon 9 between the C57BL/6 and PWK strains was used to determine the paternal allele (Fig. 1). As previously reported by Hikichi et al. (17), the major-type transcript was expressed exclusively from the maternal allele in the kidney and brain, while the brain type transcript was expressed from the paternal allele only in the brain (Fig. 3). We next examined promoter-specific imprinting in neurons, glial cells, and fibroblasts. Expression of the major-type transcript originated exclusively from the maternal allele in all cultured cells, but that of the brain type transcript detected only in neurons originated from the paternal allele (Fig. 3). Thus, predominant paternal *Grb10* expression in the brain, as previously described, can be explained by a combination of paternally expressed brain type transcript in neurons and maternally expressed major-type transcript in all cells.

Differentially methylated CGI2 is maintained in cultured neurons and glial cells. As we found that the brain type transcript was initiated from exon 1b of the paternal allele only in neurons, we analyzed the methylation status of the brain type promoter in neurons and glial cells by the bisulfite method. As shown in Fig. 4A, three promoters are located within different CGIs: exon 1a in CGI1, exon 1b in CGI2, and exon 1c in the "weaker" CpG island, CGI3. The parental origin of the methylated allele was identified by polymorphic sites in F_1 hybrids between the C57BL/6 and PWK strains. The methylation analysis of CGI2 showed that the differential methylation established in the germ cells (1, 17) was maintained in neurons and glial cells (Fig. 4B). That in other CpG islands, CGI1 and CGI3, revealed biallelic hypomethylation and hypermethylation, respectively. CGI1 and CGI3 did not show any differential methylation in the cells, although CGI3 was reported to be a putative differentially methylated region in the mouse brain with uniparental disomy for chromosome 11 (1) The methylation status in CGIs, except CGI3, in cultured cells was consistent with that previously reported for tissues (1, 17).

Parental chromosome-specific histone modifications in CGI2 correlate with allele-specific expression of the brain type transcript in neurons. Parental origin-specific histone modifications are reported to represent the determinant of epigenetic features as well as DNA methylation. Using specific antibodies against acetylated histone H3 (H3Ac), acetylated histone H4 (H4Ac), dimethylated Lys4 histone H3 (H3mK4), and di- and trimethylated Lys9 histone H3 (H3me2K9 and H3me3K9), we performed a ChIP assay with cultured cells. After evaluation of ChIP DNA by allele-specific histone modifications in the *Lit1* promoter region as a control (16), histone modifications in CGI1, CGI2, and CGI3 were analyzed by real-time PCR to quantify their precipitated chromatins in these CGIs. To normalize each value, *Gapdh* and *D13Mit55* were used as internal control sequences, where acetylated and methylated histones were known to be biallelically immunoprecipitated, depending on the corresponding antibodies. In CGI2, where the maternal allele-specific DNA methylation was established in the oocyte, H3Ac, H4Ac, H3mK4, and H3me3K9 were clearly immunoprecipitated in neurons, while in glial cells and fibroblasts, although H3mK4 and H3me3K9 were well immunoprecipitated, H3Ac and H4Ac were less precipitated (Fig. 5A). The results obtained with the antibody against H3me2K9 (data not shown) were similar to those obtained with the antibody against H3me3K9.

To elucidate the parental chromosome-specific histone modifications in CGI2 in neurons, hot-stop PCR was performed (15, 32). The restriction endonuclease Hpy188I was used to recognize the polymorphic site in CGI2. For each of the precipitated samples, the ratio of the paternal to maternal band intensities was determined. These ratios were corrected for the paternal-to-maternal ratios in the input chromatin, because the maternal and paternal alleles were not equally represented in the input chromatin. One of the parental alleles is possibly more sensitive to sonication in these regions because of relaxed chromatin (12, 16, 39). The result revealed that histones H3 and H4 were hyperacetylated and that H3K4 was hypermethylated predominantly on the paternal chromosome (Fig. 5B). To investigate allele-specific histone trimethylation of H3K9 in neurons and fibroblasts, SSCP analysis of PCR products was also performed. In

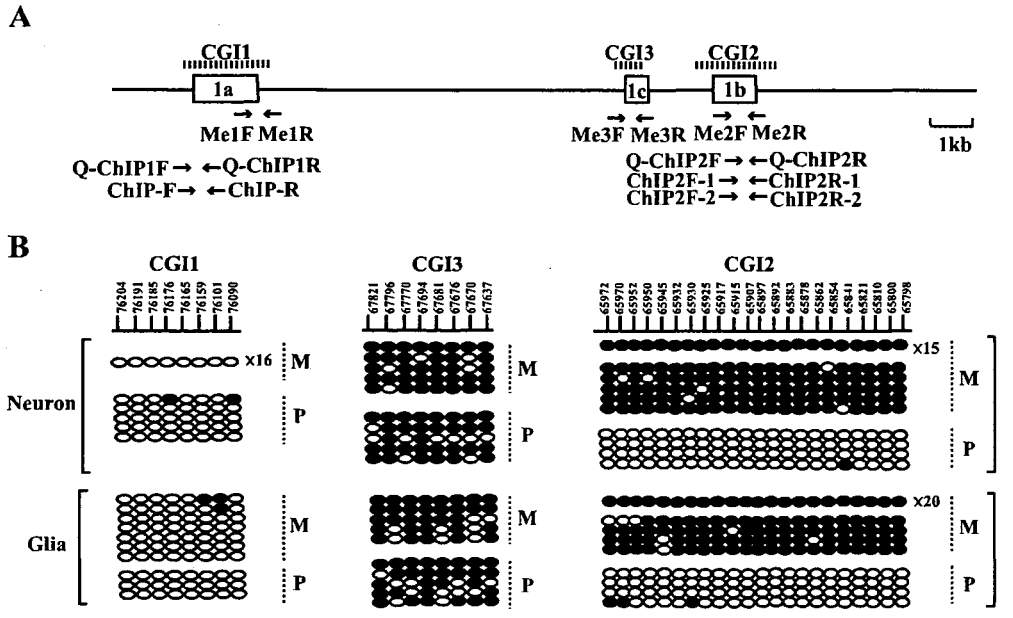

FIG. 4. Methylation status of CpG islands in neurons and glial cells. (A) Schematic structure of CpG islands. The dashed lines indicate the registered regions of CGI1, CGI2, and CGI3 (1, 17). Open boxes and arrows represent exons and primers used for methylation analysis and ChIP analysis, respectively. (B) Allele-specific DNA methylation analysis of cultured cells by bisulfite PCR and sequencing. Numbers on the line in the upper panel represent nucleotide positions, given according to GenBank accession no. AL663087. Each line shows an individual clone, and each oval represents a CpG nucleoside; the filled and open ovals indicate hypermethylated and hypomethylated CpGs, respectively. The numbers with "×" given at the right end of the clone lines represent the number of individual clones that show the same pattern of DNA methylation. Parental alleles (M, maternal; P, paternal) are distinguished by DNA polymorphisms between the C57BL/6 and PWK strains.

neurons and fibroblasts, H3K9 was hypermethylated on the maternal chromosome (Fig. 5C).

Parental chromosome-specific methylation of histone H3K27 but not H3K9 in CGI1 correlates with allele-specific expression of the major-type transcript. Histone modifications in CGI1, where CpGs were biallelically hypomethylated in tissues and cultured cells, were next analyzed. In CGI1, H3Ac, H4Ac, and H3mK4 were clearly precipitated in glial cells and fibroblasts, while the precipitations were not observed in neurons (Fig. 5A). H3me3K9 and H3me2K9 in CGI1 were not precipitated in neurons and glial cells (Fig. 5A; data not shown). The maternal chromosome-specific histone H3/H4 acetylation and H3K4 methylation in CGI1 were detected in glial cells and fibroblasts (Fig. 5D). We further analyzed histone H3K27 trimethylation, which is directly regulated by the PcG proteins, because imprinted expression of the major-type *Grb10* transcript was reported to be relaxed in the knockout embryos of the PcG gene, *Eed* (24). In neurons and fibroblasts, H3mK27 was clearly precipitated in CGI1 but not in CGI2 (Fig. 6A). The paternal chromosome-specific methylation of H3K27 was observed in fibroblasts, but a significant allelic difference was not detected in neurons (Fig. 6B). These data suggest that the paternally null expression of the major-type transcript in fibroblasts correlates with paternal chromosome-specific methylation of H3K27 in CGI1. In CGI3, histones H3 and H4 were hypoacetylated and H3K4 was hypomethylated (data not shown). We could not detect significant differences in histone acetylation and methylation in CGI3 between cultured cells.

DISCUSSION

It has been known that mouse *Grb10* shows reciprocal imprinting depending on the tissue-specific promoters. In most tissues, *Grb10* is expressed exclusively from the maternal allele, whereas in the brain, it is expressed predominantly from the paternal allele (1, 17). Such reciprocal imprinting of *Grb10* in a tissue-specific and promoter-specific manner is a good model to elucidate how promoter-specific imprinting is epigenetically controlled in tissues. In this study, we have developed a cell culture system with which cell-type-specific imprinting of *Grb10* can be characterized in the mouse brain. We demonstrated that promoter-specific and developmental stage-specific imprinting of *Grb10* expression in the brain is associated with parental allele-specific epigenetic modifications in brain cell lineages.

Two previous reports described that reciprocal imprinting of *Grb10* occurs in a tissue-specific and promoter-specific manner (1, 17). Our studies with cultured cortical cells revealed that the brain type transcript containing exon 1b was expressed in neurons but not in glial cells, while the major-type transcript containing exon 1a was expressed in all cultured cells, including neurons (Fig. 2C). These findings indicate that the brain-specific promoter actually implies the neuron-specific promoter and that the major-type promoter works as the common promoter in all tissues. Imprinting analysis of these transcripts clearly showed that the brain type transcript is expressed exclusively from the paternal allele and the major-type transcript is expressed exclusively from the maternal allele (Fig. 3). These

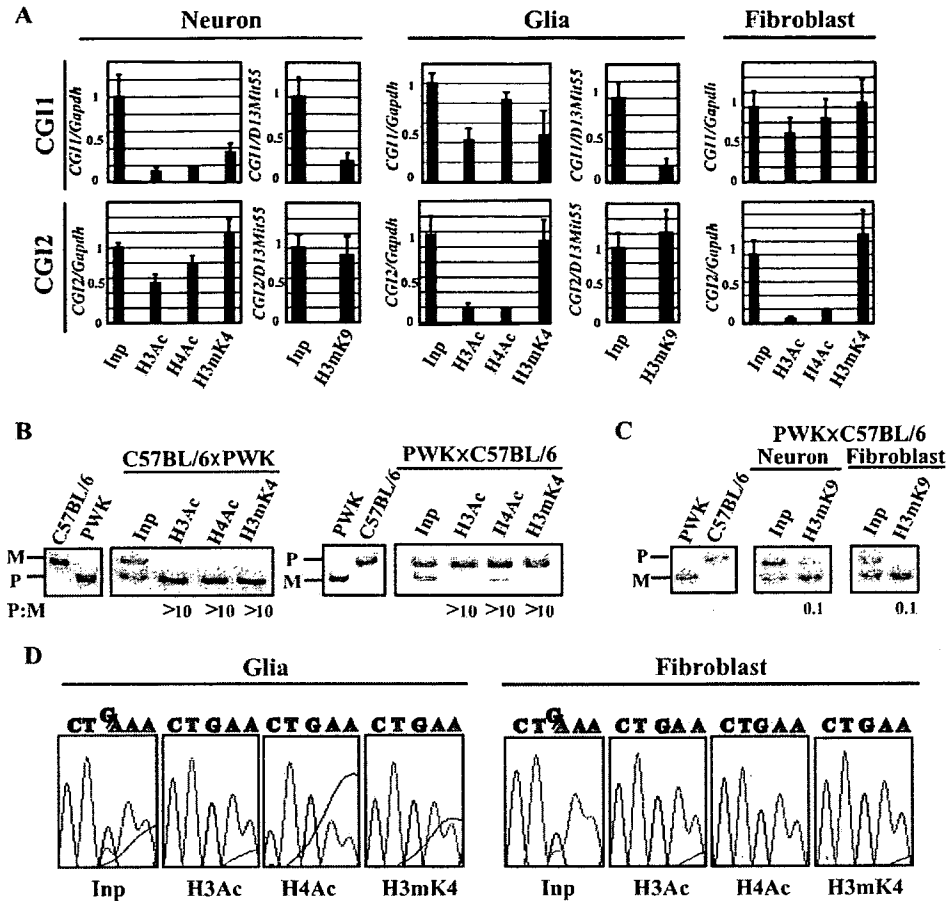

FIG. 5. Histone modification analysis of the *Grb10* promoter in cultured cells. (A) Quantitative analysis of immunoprecipitated DNA by real-time PCR. Quantitative values of precipitated DNA in CGI1 and CGI2 were normalized by dividing the average value of each CGI by the average value of *Gapdh* or *D13Mit55*. Standard errors of the means are indicated by bars. (B) Allele-specific histone modifications in CGI2 in neurons by hot-stop PCR. Digested PCR products of C57BL/6 and PWK genomic DNA are shown as homozygous controls in the first two lanes. M and P represent the products from the maternal allele and the paternal allele, respectively. The ratio of the paternal to maternal (P:M) band intensities, corrected by the ratio in input chromatin (Inp), is indicated below each lane. (C) Allele-specific histone H3K9 methylation in CGI2 by SSCP. PCR products of C57BL/6 and PWK genomic DNA were shown as controls in the first two lanes. (D) Allele-specific histone modifications in CGI1 by sequence chromatograms. Glial cells and fibroblasts derived from F_1 hybrids [(C57BL/6 × PWK)F_1] were used for analysis. The single-nucleotide (G/A) polymorphism is detected in the input sample (Inp); "G" originated from the maternal allele and "A" from the paternal allele.

results in vitro can explain the previous data that the brain type transcript was not detected in whole embryo at E9.5 (17), when neurogenesis has not yet occurred. In addition, our data on *Grb10* expression, i.e., brain development-dependent switching from the major-type to the brain type transcript, can also support the previous report that *Grb10* is expressed predominantly from the paternal allele in the adult brain (17), which consists of neurons and glial cells.

In our expression analysis, we detected both brain type and major-type transcripts in cultured neurons (Fig. 2B). Recently, it was reported that the *Pcdh* (protocadherin) gene was monoallelically expressed in individual neurons (10). The *Pcdh* gene family (*Pcdha*, *Pcdhb*, and *Pcdhc*) has variable exons and alternative splice forms. Esumi et al. analyzed the expression of transcripts in the variable exons of *Pcdha* by using a single-cell RT-PCR approach for the determination of the allelic origin for each variable exon at the individual cell level (10). The individual cells showed monoallelic expression for each variable exon. In our analysis of *Grb10*, the discrepancy between the modifications in CGI1 and the expression of the major-type transcript in neurons was recognized. Similar to a monoallelic expression pattern of variable *Pcdha* exons in individual neurons, the discrepancy may be explained by the existence of two different cell populations in cultured neurons, each of which expresses either the major-type or the brain type transcript exclusively. As shown in Fig. 2D, the brain type transcript was obviously highly expressed compared to the major-type transcript during long culture periods. The larger population of cells with the brain type transcript may affect the result of histone modifications more than the smaller population of cells with the major-type transcript.

It has been reported that histone modifications and DNA methylation are not synchronized as a transcriptionally active/silent signal in some imprinted genes, such as *NDN*, *Gnas*, and

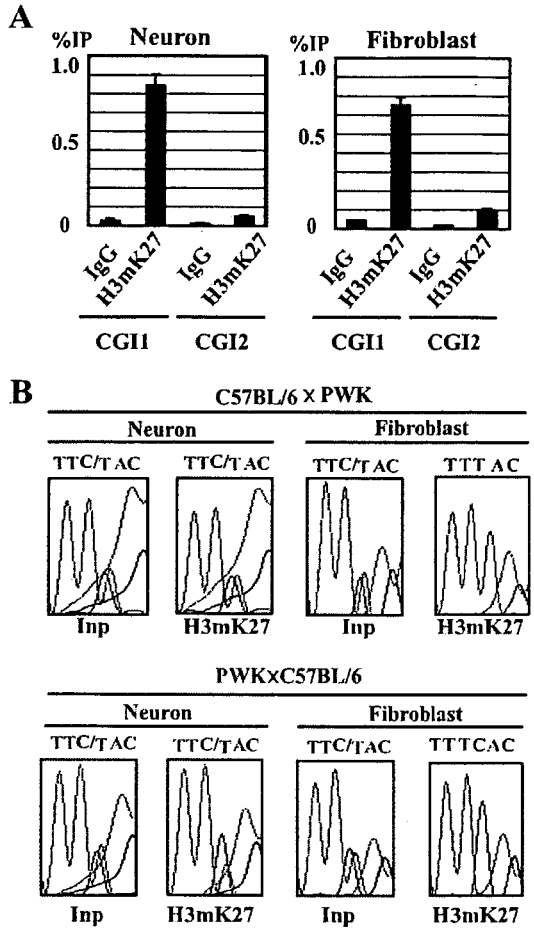

FIG. 6. Histone H3K27 methylation analysis of CGI1 and CGI2 in cultured cells. (A) Quantitative analysis of immunoprecipitated DNA by real-time PCR. The percentage of immunoprecipitation (IP) was calculated by dividing the quantitative value of precipitated DNA by that of the corresponding input DNA. Standard errors of the means are indicated by bars. (B) Allele-specific histone modifications in CGI1 by sequence chromatograms. Neurons and fibroblasts derived from F_1 hybrids (C57BL/6 × PWK; PWK × C57BL/6) were used for analysis. The single-nucleotide (C/T) polymorphism is detected in the input sample (Inp); "C" originated from the C57BL/6 allele and "T" from the PWK allele. IgG, immunoglobulin G.

Igf2r (21, 22, 23, 33, 35). Our data also showed an epigenetically unsynchronized active/silent signal between DNA methylation and histone modifications in *Grb10* (Fig. 7). In this study, we showed that the brain type transcript is expressed in neurons but not in glial cells (Fig. 2C), where both differential methylation in CGI2 and biallelic hypomethylation in CGI1 were maintained regardless of expression (Fig. 4B). The result that allele-specific DNA methylation is not sufficient to direct imprinted expression in brain cells implies that other epigenetic modifications may affect cell lineage-specific imprinting.

In our analysis of histone modifications, histone acetylation status correlated with the expression status of the major-type transcript in glial cells and fibroblasts and the brain type transcript in neurons (Fig. 7). Such histone acetylation status in *Grb10* expression is consistent with the findings that allele-specific histone acetylation was associated with allelic gene expression in the imprinted gene, *NDN* (21). Histone acetylation offers the best example of a direct link between tissue-specific gene expression and histone modifications.

Unlike that of histone acetylation, the status of histone methylation has been implicated as an early event for chromatin conformations. Methylation of histones H3K4 and H3K9 is associated with active chromatin and silent chromatin, respectively. According to our results, allele-specific H3K4 and H3K9 methylation in CGI1 and CGI2 did not correlate with allele-specific gene expression in each cultured cell. In glial cells, H3K4 in CGI2 was hypermethylated in the paternal chromosome, which was silent with no brain type transcript. It seems that H3mK4 is maintained during differentiation as an imprint mark with H3mK9 but is not related to promoter activity (28), although histone modifications in oocytes remain unknown. In CGI1, H3me2K9 and H3me3K9 were hypomethylated in both parental chromosomes independent of the expression of the major-type transcript in cultured cells. It is likely that H3K9 methylation in germ cells is maintained as a stable and heritable imprint mark but may not be secondarily acquired during development.

Then, how is maternal chromosome-specific expression of the major-type transcript regulated without differential DNA methylation in CGI1? The PcG protein Eed complex is known to be a part of a memory system that maintains repression of

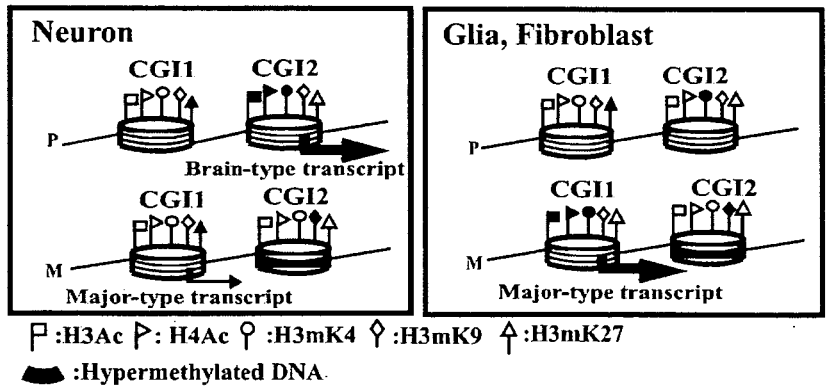

FIG. 7. Summary of epigenetic modifications across promoter regions of *Grb10*. M and P represent maternal and paternal chromosomes, respectively. Large and small arrows indicate expression levels. The nucleosome model shows DNA wrapping around a histone octamer with some histone modifications. White and black flags represent hypoacetylated/hypomethylated and hyperacetylated/hypermethylated statuses, respectively.

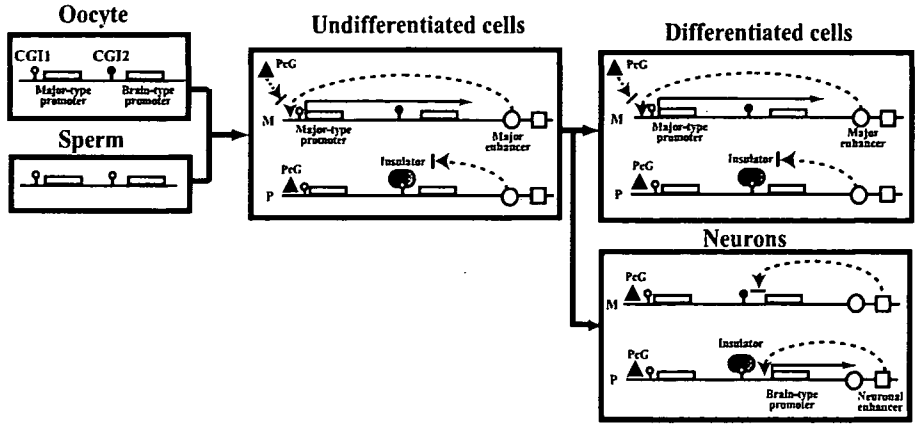

FIG. 8. Working models for tissue-specific reciprocal imprinting of *Grb10*. The previous enhancer/insulator model by Hikichi et al. was modified based on the analysis of DNA methylation and histone modifications mediated by the PcG complex containing Eed (17). Tissue-specific imprinting of *Grb10* implies neuron-specific imprinting that is different from imprinting in other undifferentiated and differentiated cells. Black and white lollipops indicate hypermethylated and hypomethylated DNA, respectively. Circles and squares indicate putative major enhancer and neuronal enhancer, respectively, which accelerate *Grb10* expression from the major-type promoter and the brain type promoter, respectively. The PcG complex containing Eed is represented by a triangle. CTCF is thought to be a putative insulator (gray oval). M, maternal; P, paternal.

the imprinted X chromosome (36) and silencing of some imprinted genes (24, 33). *Grb10* is reported to be one of the imprinted genes that are regulated by the PcG protein Eed complex. Interestingly, in $Eed^{-/-}$ embryos, the major-type transcript was biallelically expressed without major alteration of allelic DNA methylation (24). The Eed/Ezh2 PcG complex possesses histone methyltransferase activity on H3K27 (5, 8, 25) and interacts with histone deacetylases (34). Methylation of H3K27 is a repressive epigenetic mark regulated by the SET domain containing Ezh2/Eed complex (5, 8, 20, 25). In our analysis, H3mK27 was clearly precipitated in neurons and fibroblasts in CGI1 but not in CGI2 (Fig. 6A). The paternal chromosome-specific methylation of H3K27 in CGI1 was observed in fibroblasts but not in neurons (Fig. 6B). These data indicate that the Eed PcG complex can biallelically interact on CGI1 as a *trans*-acting factor in neurons but paternally in other cells. In the absence of DNA methylation in CGI1, PcG complexes may mediate a nonpermissive chromatin state for transcription, leading to repressive histone modifications. Interestingly, other genes, *Cdkn1c* and *Ascl2*, imprinting of which was reported to be regulated by Eed (24), show tissue-specific imprinting, and their imprinted expression in trophoblasts is associated with repressive histone H3K27 methylation rather than DNA methylation (22, 33).

Figure 7 shows the summary of our data. In CGI2, DNA methylation in a gametically methylated CpG island on the maternal allele was maintained throughout development. Allelic methylation of H3K4 and H3K9 associated with gametic DNA methylation was also stable as an epigenetic mark, independent of *Grb10* expression. Histone acetylation status was correlated with the expression status of the brain type transcript: histones H3 and H4 were paternally acetylated only in neurons, where the brain type transcript was paternally expressed. H3K27 was not methylated biallelically. In CGI1, biallelic DNA hypomethylation and biallelic hypomethylation of H3K9 were observed. Acetylation of histones H3 and H4 and methylation of H3K4 and H3K27 were allelically detected, corresponding to the allelic expression of the major-type transcript, although the discordance in histone modifications and expression in neurons was detected, probably depending on maturation of neurons. Methylation of H3K9 and H3K27 is thought to be a repressive chromatin marker, but it is not completely clear whether PcG-mediated silencing involves methylation of H3K9 synchronized with H3mK27 in all PcG target genes. We did not observe coexistence of H3mK27 and H3mK9 in both CGI1 and CGI2 of *Grb10*. Umlauf et al. also reported discordance between localizations of H3mK27 and H3mK9 in some imprinted genes in the *Kcnq1* domain (33). Further work should determine how histone modifications, especially methylation of H3K9 and H3K27, are coordinated or uncoordinated as epigenetic determinants in tissue-specific imprinting.

These data about epigenetic modifications analyzed at the cell level, in addition to the evidence for $Dnmt3L^{m-/-}$ and $Eed^{-/-}$ embryos, lead to a working model for tissue-specific reciprocal imprinting of *Grb10* (Fig. 8). The previous model by Hikichi et al. (17) was modified in our model based on the data of DNA methylation and repressive histone modifications mediated by the PcG complex in brain cell lineages. In undifferentiated cells, a DNA methylation-sensitive insulator, CTCF, binds to the paternal CGI2 and blocks the paternal activity of the downstream major enhancer, resulting in silent expression of the major-type transcript on the paternal allele. On the maternal allele, the major enhancer works on the major-type promoter to recruit transcription factors. In CGI1, the Eed/Ezh2 PcG complex binds on the paternal allele, whereas it competes with transcription factors on the maternal allele. The Eed/Ezh2 PcG complex methylates H3K27 and interacts with histone deacetylases, leading to silencing of the chromatin on the paternal CGI1. In $Dnmt3L^{m-/-}$ embryos, biallelic hypomethylation in CGI2 makes CTCF bind biallelically on CGI2, resulting in null expression of the major-type transcript, regardless of the PcG complex. In $Eed^{-/-}$ embryos, the silent state on the paternal CGI1 regulated by the Eed PcG complex

is released to the biallelically active state without major alteration of DNA methylation in maternal CGI2. In neurons, the other molecular mechanism of imprinting works in a promoter-specific manner, different from that in other differentiated cells. During neurogenesis, expression of *Grb10* shifts from the major-type to the brain type transcript by switching from the major-type promoter to the brain type promoter. The neuronal enhancer instead of the major enhancer may work on the brain type promoter, depending on DNA methylation in CGI2. The maternally active major-type promoter becomes silent without transcription factors, and consequently, the Eed/Ezh2 PcG complex binds to make the chromatin structure silent. This implies that the PcG complex is necessary to maintain cell-type-specific imprinting. It remains unknown how neuron-specific imprinting is regulated by DNA methylation and/or histone modifications mediated by the PcG complex, because *Dnmt3L*$^{m-/-}$ and *Eed*$^{-/-}$ embryos are lethal by E10.5 (4, 14) and E8.5 (11), respectively, just before neurogenesis.

As far as we know, this is the first report of an epigenetic analysis of cultured cells where DNA methylation and chromatin remodeling by PcG proteins establish and maintain cell-type-specific imprinting at one gene locus. Although allelic DNA methylation established in the gamete contributes primarily to tissue-specific imprinting, tissue-specific *Grb10* imprinting is directly regulated by the repressive chromatin mediated by the PcG complex during development. Our analysis of promoter-specific and cell-type-specific imprinting of *Grb10* gives an important clue for understanding the mechanism of tissue-specific imprinting.

ACKNOWLEDGMENTS

We thank F. Ishino for providing information about genomic sequences of *Grb10* promoter regions.

T.K. was supported in part by a Grant-in-Aid for Scientific Research (C) and a Grant-in-Aid on Priority Areas (Molecular Brain Science) from the Ministry of Education, Culture, Sports, Science and Technology of Japan.

REFERENCES

1. **Arnaud, P., D. Monk, M. P. Hichins, E. Gordon, W. Dean, C. Beechey, J. Peters, W. Craigen, M. Preece, P. Stanier, G. E. Moore, and G. Kelsey.** 2003. Conserved methylation imprints in the human and mouse GRB10 genes with divergent allelic expression suggests differential reading of the same mark. Hum. Mol. Genet. **12**:1005–1019.
2. **Arnaud, P., K. Hata, M. Kaneda, E. Li, H. Sasaki, R. Feil, and G. Kelsey.** 2006. Stochastic imprinting in the progeny of Dnmt3L−/− females. Hum. Mol. Genet. **15**:589–598.
3. **Bantignies, F., and G. Cavalli.** 2006. Cellular memory and dynamic regulation of Polycomb group proteins. Curr. Opin. Cell Biol. **18**:1–9.
4. **Bourc'his, D., G. L. Xu, C. S. Lin, B. Bollman, and T. H. Bester.** 2001. Dnmt3L and the establishment of maternal genomic imprints. Science **294**: 2536–2539.
5. **Cao, R., L. Wang, H. Wang, L. Xia, H. Erdjument-Bromage, P. Tempst, R. S. Jones, and Y. Zhang.** 2002. Role of histone H3 lysine 27 methylation in Polycomb-group silencing. Science **298**:1039–1043.
6. **Cattanach, B. M., and C. V. Beechey.** 1990. Autosomal and X-chromosome imprinting. Dev. Suppl. **1990**:63–72.
7. **Constancia, M., B. Pickard, G. Kelsey, and W. Reik.** 1988. Imprinting mechanisms. Genome Res. **8**:881–900.
8. **Czermin, B., R. Melfi, D. McCabe, V. Seitz, A. Imhof, and V. Pirrotta.** 2002. Drosophila enhancer of Zeste/ESC complexes have a histone H3 methyltransferase activity that marks chromosomal Polycomb sites. Cell **111**:185–196.
9. **Davies, W., A. R. Isles, and L. S. Wilkinson.** 2005. Imprinted gene expression in the brain. Neurosci. Biobehav. Rev. **29**:421–430.
10. **Esumi, S., N. Kakazu, Y. Taguchi, T. Hirayama, A. Sasaki, T. Hirabayashi, T. Koide, T. Kitsukawa, S. Hamada, and T. Yagi.** 2005. Monoallelic yet combinatorial expression of variable exons of the protocadherin-α gene cluster in single neurons. Nat. Genet. **37**:171–176.
11. **Faust, C., A. Schumacher, B. Holdener, and T. Magnuson.** 1995. The eed mutation disrupts anterior mesoderm production in mice. Development **121**: 273–285.
12. **Fournier, C., Y. Goto, E. Ballestar, K. Delaval, A. M. Hever, M. Esteller, and R. Feil.** 2002. Allele-specific histone lysine methylation marks regulatory regions at imprinted mouse genes. EMBO J. **21**:6560–6570.
13. **Gregory, R. I., T. E. Randall, C. A. Johnson, S. Khosla, I. Hatada, L. P. O'Neill, B. M. Turner, and R. Feil.** 2001. DNA methylation is linked to deacethylation of histone H3, but not H4, on the imprinted genes *Snrpn* and *U2af1-rs1*. Mol. Cell. Biol. **21**:5426–5436.
14. **Hata, K., M. Okano, H. Lei, and E. Li.** 2002. Dnmt3L cooperates with the Dnmt3 family of de novo DNA methyltransferases to establish maternal imprints in mice. Development **129**:1983–1993.
15. **Higashimoto, K., H. Soejima, H. Yatsuki, K. Joh, M. Uchiyama, Y. Obata, R. Ono, Y. Wang, Z. Xin, X. Zhu, S. Masuko, F. Ishino, I. Hatada, Y. Jinno, T. Iwasaka, T. Katsuki, and T. Mukai.** 2002. Characterization and imprinting status of *OBPH1/Obph1* gene: implications for an extended imprinting domain in human and mouse. Genomics **80**:575–584.
16. **Higashimoto, K., T. Urano, K. Sugiura, H. Yatsuki, K. Joh, W. Zhao, M. Iwakawa, H. Ohashi, M. Oshimura, N. Niikawa, T. Mukai, and H. Soejima.** 2003. Loss of CpG methylation is strongly correlated with loss of histone H3 lysine 9 methylation at DMR-LIT1 in patients with Beckwith-Wiedemann syndrome. Am. J. Hum. Genet. **73**:948–956.
17. **Hikichi, T., T. Kohda, T. Kaneko-Ishino, and F. Ishino.** 2003. Imprinting regulation of the murine *Meg1/Grb10* and human *GRB10* genes; roles of brain-specific promoters and mouse-specific CTCF-binding sites. Nucleic Acids Res. **31**:1398–1406.
18. **Kaneda, M., M. Okano, K. Hata, T. Sado, N. Tsujimoto, E. Li, and H. Sasaki.** 2004. Essential role for de novo DNA methyltransferase Dnmt3a in paternal and maternal imprinting. Nature **429**:900–903.
19. **Kishino, T.** 2006. Imprinting in neurons. Cytogenet. Genome Res. **113**:209–214.
20. **Kuzmichev, A., K. Nishioka, H. Erdjument-Bromage, P. Tempst, and D. Reinberg.** 2002. Histone methyltransferase activity associated with a human multiprotein complex containing the Enhancer of Zeste protein. Genes Dev. **16**:2893–2905.
21. **Lau, J. C., M. L. Hanel, and R. Wevrick.** 2004. Tissue-specific and imprinted epigenetic modifications of the human *NDN* gene. Nucleic Acids Res. **32**: 3376–3382.
22. **Lewis, A., K. Mitsuya, D. Umlauf, P. Smith, W. Dean, J. Walter, M. Higgins, R. Feil, and W. Reik.** 2004. Imprinting on distal chromosome 7 in the placenta involves repressive histone methylation independent of DNA methylation. Nat. Genet. **36**:1291–1295.
23. **Li, T., T. H. Vu, G. A. Ulaner, Y. Yang, J. F. Hu, and A. R. Hoffman.** 2004. Activating and silencing histone modifications from independent allelic switch regions in the imprinted *Gnas* gene. Hum. Mol. Genet. **13**:741–750.
24. **Mager, J., N. D. Montgomery, F. P. de Villena, and T. Magnuson.** 2003. Genome imprinting regulated by the mouse Polycomb group protein Eed. Nat. Genet. **33**:502–507.
25. **Muller, J., C. M. Hart, N. J. Francis, M. L. Vargas, A. Sengupta, B. Wild, E. L. Miller, M. B. O'Connor, R. E. Kingston, and J. A. Simon.** 2002. Histone methyltransferase activity of a Drosophila Polycomb group repressor complex. Cell **111**:197–208.
26. **Nakagawachi, T., H. Soejima, T. Urano, W. Zhao, K. Higashimoto, Y. Satoh, S. Matsukura, S. Kudo, Y. Kitajima, H. Harada, K. Furukawa, H. Matsuzaki, M. Emi, Y. Nakabeppu, K. Miyazaki, M. Sekiguchi, and T. Mukai.** 2003. Silencing effect of CpG island hypermethylation and histone modifications on O6-methylguanine-DNA methyltransferase (*MGMT*) gene expression in human cancer. Oncogene **22**:8835–8844.
27. **Pirrotta, V.** 1995. Chromatin complexes regulating gene expression in Drosophila. Curr. Opin. Genet. Dev. **5**:466–472.
28. **Rougeulle, C., P. Navarro, and P. Avner.** 2003. Promoter-restricted H3 Lys 4 di-methylation is an epigenetic mark for monoallelic expression. Hum. Mol. Genet. **12**:3343–3348.
29. **Saitoh, S., and T. Wada.** 2000. Parent-of-origin specific histone acetylation and reactivation of a key imprinted gene locus in Prader-Willi syndrome. Am. J. Hum. Genet. **66**:1958–1962.
30. **Surani, M. A., S. C. Barton, and M. L. Norris.** 1984. Development of reconstituted mouse eggs suggests imprinting of the genome during gametogenesis. Nature **308**:548–550.
31. **Tilghman, S. M.** 1999. The sins of the fathers and mothers: genomic imprinting in mammalian development. Cell **96**:185–193.
32. **Uejima, H., M. P. Lee, H. Cui, and A. P. Feinberg.** 2000. Hot-stop PCR: a simple and general assay for linear quantitation of allele ratios. Nat. Genet. **25**:375–376.
33. **Umlauf, D., Y. Goto, R. Cao, F. Cerqueira, A. Wagschal, Y. Zhang, and R. Feil.** 2004. Imprinting along the *Kcnq1* domain on mouse chromosome 7 involves repressive histone methylation and recruitment of Polycomb group complexes. Nat. Genet. **36**:1296–1300.
34. **van der Vlag, J., and A. P. Otte.** 1999. Transcriptional repression mediated by the human polycomb-group protein EED involves histone deacetylation. Nat. Genet. **23**:474–478.
35. **Vu, T. H., T. Li, and A. R. Hoffman.** 2004. Promoter-restricted histone code,